

# Constrained Secrecy Capacity of Partial-Response Wiretap Channels

Aria Nouri, *Student Member, IEEE*, Reza Asvadi, *Senior Member, IEEE*,  
Jun Chen, *Senior Member, IEEE*, and Pascal O. Vontobel, *Fellow, IEEE*

## Abstract

We consider reliable and secure communication over partial-response wiretap channels (PR-WTCs). In particular, we first examine the setup where the source at the input of a PR-WTC is unconstrained and then, based on a general achievability result for arbitrary wiretap channels, we derive an achievable secure information rate for this PR-WTC. Afterwards, we examine the setup where the source at the input of a PR-WTC is constrained to be a finite-state machine source (FSMS) of a certain order and structure. Optimizing the parameters of this FSMS toward maximizing the secure information rate is a computationally intractable problem in general, and so, toward finding a local maximum, we propose an iterative algorithm that at every iteration replaces the secure information rate function by a suitable surrogate function whose maximum can be found efficiently. Although we expect the secure information rates achieved in the unconstrained setup to be larger than the secure information rates achieved in the constrained setup, the latter setup has the advantage of leading to efficient algorithms for estimating achievable secure rates and also has the benefit of being the basis of efficient encoding and decoding schemes.

## Index Terms

Partial-response wiretap channel (PR-WTC), finite-state machine channel, finite-state machine source, wiretap channel, secure rate, rate optimization.

A. Nouri and R. Asvadi are with the Cognitive Telecommunication Research Group, Department of Telecommunications, Faculty of Electrical Engineering, Shahid Beheshti University, Tehran, Iran. (e-mails: ar.nouri@mail.sbu.ac.ir; r\_asvadi@sbu.ac.ir) R. Asvadi is the corresponding author.

J. Chen is with the Department of Electrical and Computer Engineering, McMaster University, Hamilton, ON, Canada (e-mail: junchen@mail.ece.mcmaster.ca).

P.O. Vontobel is with the Department of Information Engineering and the Institute of Theoretical Computer Science and Communications, The Chinese University of Hong Kong, Hong Kong SAR (e-mail: pascal.vontobel@ieee.org).

## I. INTRODUCTION

### A. Background

Partial-response (PR) channels are a class of channels with memory that are used as a model for transmission over bandwidth-limited channels. These channels are useful models in many applications including data storage and magnetic recording [1]–[3], wireless communication over time-varying multipath channels [4], optical communications and digital subscriber lines [5]. PR channels are a special case of finite-state machine channels (FSMCs), sometimes also called finite-state channels (FSCs) [6]. Deriving upper and lower bounds on the capacity of FSMCs has received significant attention in order to design and evaluate codes for such channels [7].

The classical Blahut-Arimoto algorithm (BAA) [8], [9] was generalized in [10] to optimize finite-state machine sources (FSMSs) at the input of FSMCs in order to maximize the mutual information rate between channel input and output. A comparison of achievable information rates [10], [11] with upper bounds on the (unconstrained) capacity of FSMCs [12], [13] shows that typically there exists only a small gap between them, a gap that can be further narrowed by increasing the memory length of the FSMSs [14]. Hence, the information rates achievable with FSMSs at the input of FSMCs are close to optimal.

Inherent non-ideal properties of communication channels, such as noise and interference, can be exploited for achieving security at the physical layer. Information-theoretic limits of secure communications without a secret key agreement between a transmitter and a legitimate receiver was first considered in [15], [16]. The ubiquity of PR channels in communications and a growing demand for physical layer secrecy has led to increased attention to the analysis of the secrecy capacity of PR-wiretap channels (PR-WTCs). A PR-WTC consists of a primary channel and a secondary channel, where the primary channel is a PR channel that connects a transmitter (Alice) to a legitimate receiver (Bob), and where the secondary channel is a PR channel that connects the transmitter (Alice) to an eavesdropper (Eve). In the following, the primary channel will be called “Bob’s channel” and labeled “B”, whereas the secondary channel will be called “Eve’s channel” and labeled “E”.

In [17], useful secrecy metrics have been introduced based on distances between two random variables, corresponding to a transmitted message and Eve’s observation of it,

respectively. The distances are ordered with respect to (w.r.t.) their strength in guaranteeing secrecy over a wiretap channel. By using these metrics and channel resolvability techniques, the results of secrecy capacity for discrete memoryless wiretap channels (DM-WTCs) have been generalized to arbitrary wiretap channels [18].

### B. Contribution

In this paper, we consider a PR-WTC *without* feedback, where the input symbols are limited to some finite alphabet. In a first step, we study the *unconstrained* setup, i.e., the setup where no constraints are placed on Alice's source, and derive an achievable secure information rate based on the general achievability result for arbitrary wiretap channels established using information-spectrum methods [19]. Afterwards, we consider the *constrained* setup, i.e., the setup where Alice's source is an FSMS of a given order and structure, and propose an efficient iterative algorithm for optimizing the parameters of this FSMS toward (locally) maximizing the above-mentioned achievable secure information rate. The key idea behind this algorithm is to approximate the secure information rate by suitable surrogate functions that can relatively easily be maximized. The proposed algorithm resembles the well-known expectation-maximization (EM) algorithm and has similar convergence behavior. Moreover, its searching step size can be controlled via two adjustable parameters.

Roughly speaking, the FSMS that is found by this algorithm is the FSMS of a given order and structure that best exploits the discrepancies between the frequency responses of Bob's channel and Eve's channel. Numerical simulations indicate that the obtained secrecy capacities can be positive even for scenarios where the capacity of Eve's channel is higher than the capacity of Bob's channel.

### C. Related Work

In terms of the main focus of this paper, i.e., the secrecy capacity of PR-WTCs *without* feedback, to the best of our knowledge, the only prior work can be found in [20]. Namely, in that paper the authors consider the problem of evaluating the secrecy capacity of a finite-state wiretap channel (FS-WTC). The FS-WTC is defined as a wiretap channel where Bob and Eve observe the input source through two distinct FSMCs. Based on general results of

the DM-WTCs and imposing the less noisier condition on Bob's channel (compared with Eve's channel), the authors in [20] generalized the expression of the secrecy capacity of DM-WTCs to the case of FS-WTCs. Then, they apply a stochastic algorithm to approximate this quantity. This approach has the following issues:

- They derived the secrecy capacity of FS-WTCs based on the general results of DM-WTCs. In DM-WTCs, it is necessary to impose a so-called less-noisier constraint on Bob's channel compared with Eve's channel in order to relate the secure information rate of the wiretap channel to the information rates of Bob's and Eve's channels. However, channels with different non-flat frequency responses cannot be ordered by their noise power. Even if we could order the channels based on their unconstrained capacities, we demonstrate in our simulations that positive secure rates are achievable for the cases that Bob's channel has lower unconstrained channel capacity compared with Eve's channel.
- Another issue in their proposed algorithm is their choice of function approximating the secure information rate function. The gradient of this approximating function at an operating point is not the same as the gradient of the secure rate function at that point. This issue leads to an inaccurate search direction, which eventually makes the algorithm unstable.
- They only discuss PR channels as an example of an FSMC. In fact, they do not show simulation results corresponding to PR channels or other FSMCs. (The simulation results that are shown in [20] correspond to the maximized secure information rate of the wiretap channel comprised of a *noiseless* channel to Bob and a *binary symmetric channel* to Eve (see [20, Fig. 2]). The achievable secure rate of this wiretap channel is maximized by optimizing the parameters of a run-length constrained Markov source [10, *Example 17*] as an input source.)

The secrecy capacity of finite-state Markov wiretap channels<sup>1</sup> *with* delayed noiseless feedback from the legitimate receiver to the transmitter has recently been studied in [21], [22]. The feedback information contains the received output and the state of Bob's channel. It

<sup>1</sup>In the terminology of the present paper, a Markov wiretap channel is a wiretap channel where Bob's and Eve's channels are FSMCs with a state process that evolves independently of the input process.

is shown in [21] that such feedback can enlarge the rate-equivocation region for finite-state Markov wiretap channels compared with the case without feedback. It is also known that higher secure rates can be achieved by introducing artificial noise matched to the spectrum of Bob's channel [23]. Although these enhancements are certainly interesting, in this paper we focus on the standard version of the PR-WTC model (with neither feedback nor additional artificial noise) as it requires few assumptions and consequently is more practically relevant.

#### D. Paper Organization

The remainder of this paper is organized as follows. Sections II-A and II-B introduce the system model and some preliminary concepts related to PR-WTCs, FSMSs, and FSMCs. Section II-C presents achievability results on the (unconstrained and constrained) secure information rate of PR-WTCs. Section III discusses an efficient algorithm for estimating the secure rate for a given FSMS at the input of a PR-WTC. Section IV describes the algorithm mentioned in Section I-B for optimizing the FSMS at the input of a PR-WTC and analyzes it in detail. Section V contains some numerical results and discussions. Finally, Section VI draws the conclusion.

#### E. Notation

The sets of integers and real numbers are denoted by  $\mathbb{Z}$  and  $\mathbb{R}$ , respectively. Other than that, sets are denoted by calligraphic letters, e.g.,  $\mathcal{S}$ . The Cartesian product of two sets  $\mathcal{X}$  and  $\mathcal{Y}$  is written as  $\mathcal{X} \times \mathcal{Y}$ , and the  $n$ -fold Cartesian product of  $\mathcal{X}$  with itself is written as  $\mathcal{X}^n$ . If  $\mathcal{X}$  is a finite set, then its cardinality is denoted by  $|\mathcal{X}|$ .

Random variables are denoted by upper-case italic letters, e.g.,  $X$ , their realizations by the corresponding lower-case letters, e.g.,  $x$ , and the set of possible values by the corresponding calligraphic letter, e.g.,  $\mathcal{X}$ . Random vectors are denoted by upper-case boldface letters, e.g.,  $\mathbf{X}$ , and their realizations by the corresponding lower-case letters, e.g.,  $\mathbf{x}$ . For integers  $n_1$  and  $n_2$  satisfying  $n_1 \leq n_2$ , the notation  $\mathbf{X}_{n_1}^{n_2} \triangleq (X_{n_1}, X_{n_1+1}, \dots, X_{n_2})$  is used for a time-indexed vector of random variables and  $\mathbf{x}_{n_1}^{n_2} \triangleq (x_{n_1}, x_{n_1+1}, \dots, x_{n_2})$  for its realization.

The probability of an event  $\xi$  is denoted by  $\Pr(\xi)$ . Furthermore,  $p_X(\cdot)$  denotes the probability mass function (PMF) of  $X$  if  $X$  is a discrete random variable and the probability

density function (PDF) of  $X$  if  $X$  is a continuous random variable. Similarly,  $p_{Y|X}(\cdot|x)$  denotes the conditional PMF of  $Y$  given  $X = x$  if  $Y$  is a discrete random variable and the conditional PDF of  $Y$  given  $X = x$  if  $Y$  is a continuous random variable.

Note that boldface letters are also used for (deterministic) matrices, e.g.,  $\mathbf{A}$ , with the  $(i,j)$ -entry of  $\mathbf{A}$  being called  $A_{ij}$ .

The function  $\log(\cdot)$  denotes the natural logarithm. The entropy of a random variable  $X$ , the mutual information between two random variables  $X$  and  $Y$ , and the mutual information between two random variables  $X$  and  $Y$  conditioned on the random variable  $Z$  are denoted by  $H(X)$ ,  $I(X;Y)$ , and  $I(X;Y|Z)$ , respectively. The *information density* between the respective realizations of random variables  $X$  and  $Y$  is defined to be

$$i(x; y) \triangleq \log \left( \frac{p_{X,Y}(x, y)}{p_X(x) \cdot p_Y(y)} \right).$$

Moreover, the *conditional information density* between the respective realizations of random variables  $X$  and  $Y$  given  $Z = z$  is

$$i(x; y|z) \triangleq \log \left( \frac{p_{X,Y|Z}(x, y|z)}{p_{X|Z}(x|z) \cdot p_{Y|Z}(y|z)} \right).$$

Note that

$$I(X; Y) = \sum_{x,y} p_{X,Y}(x, y) \cdot i(x; y),$$

$$I(X; Y|Z) = \sum_{x,y,z} p_{X,Y,Z}(x, y, z) \cdot i(x; y|z).$$

Finally, the variational distance between the PMFs of two random variables  $X$  and  $Y$  over the same finite alphabet  $\mathcal{X}$  is defined as  $d_{\mathcal{X}}(p_X, p_Y) \triangleq \sum_{x \in \mathcal{X}} |p_X(x) - p_Y(x)|$ .

## II. SYSTEM MODEL AND INFORMATION RATES

Section II-A gives the definitions of finite-state machine sources (FSMSs) and finite-state machine channels (FSMCs), based on which Section II-B defines finite-state joint source-wiretap channels (FS-JWCs). Various information rates relevant for FS-JWCs are then introduced and characterized in Section II-C.

### A. Finite-State Machine Sources and Channels

In this section, we define finite-state machine sources and finite-state machine channels, along with special cases of such sources and channels as far as relevant for this paper. For more background and more examples we refer the interested reader to [6], [10].

*Definition 1 (Finite-state machine source (FSMS)).* A time-invariant (discrete-time) FSMS has a state process  $\{\bar{S}_t\}_{t \in \mathbb{Z}}$  and an output process  $\{X_t\}_{t \in \mathbb{Z}}$ , where  $\bar{S}_t \in \bar{\mathcal{S}}$  and  $X_t \in \mathcal{X}$  for all  $t \in \mathbb{Z}$ . We assume that the alphabets  $\bar{\mathcal{S}}$  and  $\mathcal{X}$  are finite and that for any positive integer  $n$  the joint PMF of  $\bar{\mathbf{S}}_1^n$  and  $\mathbf{X}_1^n$  conditioned on  $\bar{S}_0 = \bar{s}_0$  decomposes as

$$p_{\mathbf{X}_1^n, \bar{\mathbf{S}}_1^n | \mathbf{s}_0}(\mathbf{x}_1^n, \bar{\mathbf{s}}_0^n | \mathbf{s}_0) = \prod_{t=1}^n p_{X_t, \bar{S}_t | \bar{S}_{t-1}}(x_t, \bar{s}_t | \bar{s}_{t-1}),$$

where  $p_{X_t, \bar{S}_t | \bar{S}_{t-1}}(x_t, \bar{s}_t | \bar{s}_{t-1})$  is independent of  $t$ .  $\square$

*Remark 2.* In the following, we will mostly consider FSMSs where  $\bar{\mathcal{S}} \triangleq \mathcal{X}^{\bar{\nu}}$  for some positive integer  $\bar{\nu}$  and  $\bar{s}_t \triangleq \mathbf{x}_{t-\bar{\nu}+1}^t$  for all  $t \in \mathbb{Z}$ . Note:

- The integer  $\bar{\nu}$  will be called the memory order of such an FSMS.
- It holds that

$$p_{X_t, \bar{S}_t | \bar{S}_{t-1}}(x_t, \bar{s}_t | \bar{s}_{t-1}) = p_{X_t | \bar{S}_{t-1}}(x_t | \bar{s}_{t-1}) = p_{X_t | X_{t-\bar{\nu}}^{t-1}}(x_t | \mathbf{x}_{t-\bar{\nu}}^{t-1}),$$

for  $\bar{s}_t = \mathbf{x}_{t-\bar{\nu}+1}^t$  and  $\bar{s}_{t-1} = \mathbf{x}_{t-\bar{\nu}}^{t-1}$ .

- There is a bijection between state sequences and output sequences, i.e., one sequence determines the other sequence.

From the above comments it follows that such an FSMS is characterized by the triple  $(\mathcal{X}, \bar{\nu}, p_{X_t | X_{t-\bar{\nu}}^{t-1}}(x_t | \mathbf{x}_{t-\bar{\nu}}^{t-1}))$ .  $\square$

Note that all possible state sequences of an FSMS can be represented by a trellis diagram. Because of the assumed time-invariance, it is sufficient to show a single trellis section. For example, Fig. 1(a) shows a trellis section for an FSMS characterized by the triple  $(\mathcal{X} \triangleq \{+1, -1\}, \bar{\nu} \triangleq 3, p_{X_t | X_{t-\bar{\nu}}^{t-1}}(x_t | \mathbf{x}_{t-\bar{\nu}}^{t-1}))$ .

Before giving the definition of a partial-response (PR) channel, which is the type of channel of main interest in this paper, we introduce the more general class of finite-state machine channels (which were called finite-state channels in [6]).

*Definition 3 (Finite-state machine channel (FSMC)).* A time-invariant FSMC has an input process  $\{X_t\}_{t \in \mathbb{Z}}$ , an output process  $\{Y_t\}_{t \in \mathbb{Z}}$ , and a state process  $\{S'_t\}_{t \in \mathbb{Z}}$ , where  $X_t \in \mathcal{X}$ ,  $Y_t \in \mathcal{Y}$ , and  $S'_t \in \mathcal{S}'$  for all  $t \in \mathbb{Z}$ . We assume that the alphabets  $\mathcal{X}$  and  $\mathcal{S}'$  are finite and that for any positive integer  $n$  the joint PMF/PDF of  $\mathbf{S}'_1^n$  and  $\mathbf{Y}_1^n$  conditioned on  $S'_0 = s'_0$  and  $\mathbf{X}_1^n = \mathbf{x}_1^n$  is

$$p_{\mathbf{S}'_1^n, \mathbf{Y}_1^n | S'_0, \mathbf{X}_1^n}(\mathbf{s}'_1^n, \mathbf{y}_1^n | s'_0, \mathbf{x}_1^n) = \prod_{t=1}^n p_{S'_t, Y_t | S'_{t-1}, X_t}(s'_t, y_t | s'_{t-1}, x_t),$$

where  $p_{S'_t, Y_t | S'_{t-1}, X_t}(s'_t, y_t | s'_{t-1}, x_t)$  is independent of  $t$ .  $\square$

An important special case of an FSMC is a partial-response (PR) channel.

*Definition 4 (Partial-response (PR) channel).* A PR channel with transfer polynomial  $g(D) \triangleq \sum_{t=0}^m g_t D^t \in \mathbb{R}[D]$ , where  $m$  is called the memory length, has an input process  $\{X_t\}_{t \in \mathbb{Z}}$ , a noiseless output process  $\{U_t\}_{t \in \mathbb{Z}}$  and a noisy output process  $\{Y_t\}_{t \in \mathbb{Z}}$ ,

$$\begin{aligned} U_t &\triangleq \sum_{\ell=0}^m g_\ell X_{t-\ell}, \quad t \in \mathbb{Z}, \\ Y_t &\triangleq U_t + N_t, \quad t \in \mathbb{Z}, \end{aligned}$$

where  $X_t, U_t, Y_t \in \mathbb{R}$  for all  $t \in \mathbb{Z}$ . In the following, we will assume that the noise process is white Gaussian noise, i.e.,  $\{N_t\}_{t \in \mathbb{Z}}$  are i.i.d. Gaussian random variables with mean zero and variance  $\sigma^2$ . Clearly, a PR channel is parameterized by the couple  $(g(D), \sigma^2)$ .  $\square$

A PR channel described by the couple  $(g(D) \triangleq \sum_{t=0}^m g_t D^t, \sigma^2)$  and having an input process  $\{X_t\}_{t \in \mathbb{Z}}$  taking values in a finite set  $\mathcal{X} \subsetneq \mathbb{R}$ , is a special case of an FSMC. Indeed, let  $\mathcal{S}' \triangleq \mathcal{X}^m$ . Then

$$p_{S'_t, Y_t | S'_{t-1}, X_t}(s'_t, y_t | s'_{t-1}, x_t) = p_{S'_t | S'_{t-1}, X_t}(s'_t | s'_{t-1}, x_t) \cdot p_{Y_t | S'_{t-1}, X_t}(y_t | s'_{t-1}, x_t),$$

where

$$\begin{aligned} p_{S'_t | S'_{t-1}, X_t}(s'_t | s'_{t-1}, x_t) &\triangleq \begin{cases} 1 & (\text{if } s'_t = \mathbf{x}_{t-m+1}^t \text{ and } s'_{t-1} = \mathbf{x}_{t-m}^{t-1}) \\ 0 & (\text{otherwise}) \end{cases}, \\ p_{Y_t | S'_{t-1}, X_t}(y_t | s'_{t-1}, x_t) &\triangleq \frac{1}{\sqrt{2\pi\sigma^2}} \cdot \exp\left(-\frac{(y_t - u_t)^2}{2\sigma^2}\right), \end{aligned}$$

and where  $u_t \triangleq \sum_{\ell=0}^m g_\ell x_{t-\ell}$  with  $\mathbf{x}_{t-m}^{t-1} = s'_{t-1}$ .

All possible state sequences of a PR channel (and, more generally, of an FSMC) can be represented by a trellis diagram. Because of the assumed time-invariance, it is sufficient to show a single trellis section. For example, Fig. 1(b) shows a trellis section for a PR channel characterized by the couple  $(g(D) \triangleq 1 - D, \sigma^2)$  (known as a dicode channel) and with input alphabet  $\mathcal{X} \triangleq \{+1, -1\}$ . In this diagram, branches start at state  $s'_{t-1}$ , end at state  $s'_t$ , and have noiseless channel output symbol  $u_t$  shown next to them.

We are now ready to define the type of wiretap channel of interest in this paper.

*Definition 5 (Partial-response wiretap channel (PR-WTC)).* In a PR-WTC, Alice transmits data symbols over Bob's channel and over Eve's channel, which are both assumed to be PR channels with finite input alphabet  $\mathcal{X} \subseteq \mathbb{R}$ . Specifically, Bob's channel is a PR channel described by the couple  $(g^B(D), \sigma_B^2)$ , with transfer polynomial  $g^B(D) = \sum_{t=0}^{m_B} g_t^B D^t$ , noiseless output process  $\{U_t\}_{t \in \mathbb{Z}}$ , noise process  $\{N_t^B\}_{t \in \mathbb{Z}}$ , and noisy output process  $\{Y_t\}_{t \in \mathbb{Z}}$ . Similarly, Eve's channel is a PR channel described by the couple  $(g^E(D), \sigma_E^2)$ , with transfer polynomial  $g^E(D) = \sum_{t=0}^{m_E} g_t^E D^t$ , noiseless output process  $\{V_t\}_{t \in \mathbb{Z}}$ , noise process  $\{N_t^E\}_{t \in \mathbb{Z}}$ , and noisy output process  $\{Z_t\}_{t \in \mathbb{Z}}$ . We assume that the noise process of Bob's channel and the noise process of Eve's channel are independent. Clearly, the PR-WTC is parameterized by the quadruple  $(g^B(D), g^E(D), \sigma_B^2, \sigma_E^2)$ .  $\square$

### B. Finite-State Joint Source-Wiretap Channels

*Definition 6.* We define a finite-state joint source wiretap channel (FS-JSWTC) model based on the concatenation of the following components:

- an FSMS as in Remark 2 described by the triple  $(\mathcal{X}, \bar{\nu}, p_{X_t|X_{t-\bar{\nu}}^{t-1}}(x_t|\mathbf{x}_{t-\bar{\nu}}^{t-1}))$ , where  $\mathcal{X}$  is a finite subset of  $\mathbb{R}$ ;
- a PR-WTC as in Definition 5 described by the quadruple  $(g^B(D), g^E(D), \sigma_B^2, \sigma_E^2)$ .

$\square$

Note that an FS-JSWTC can be modeled by a single (time-invariant) finite-state machine. Namely, letting

$$\nu \triangleq \max(\bar{\nu}, m_B, m_E), \quad (1)$$

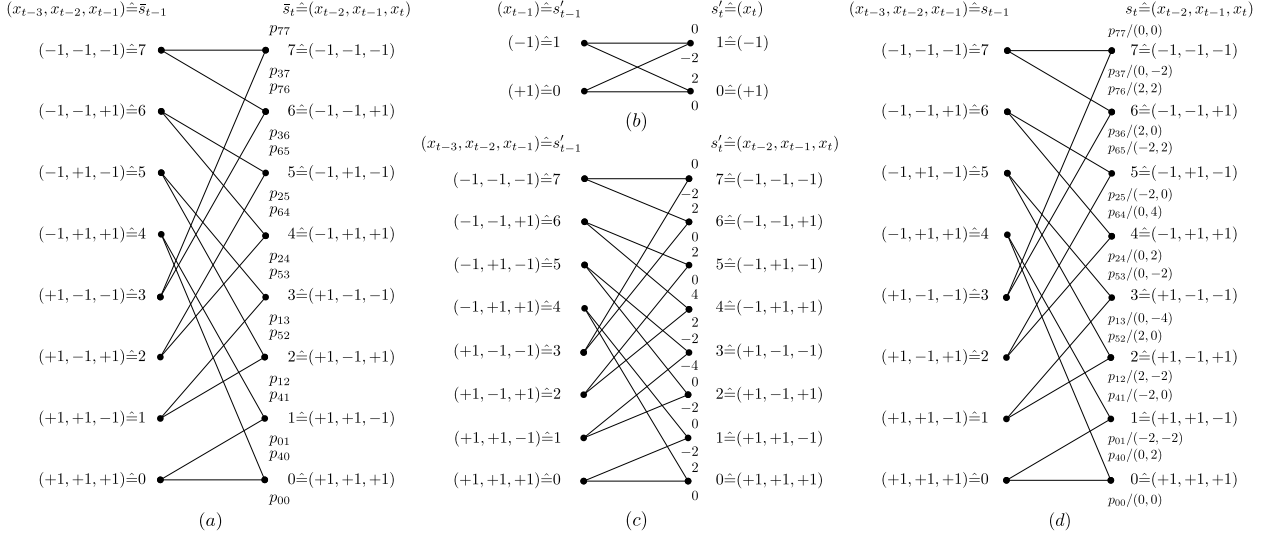


Fig. 1: (a) Trellis section of an FSMS with  $\mathcal{X} = \{+1, -1\}$  and memory order  $\bar{\nu} = 3$ . State transition probabilities are shown next to branches. (b) Trellis section of a dicode channel (i.e., a PR channel with  $g(D) = 1 - D$ ) when used with input alphabet  $\mathcal{X} = \{+1, -1\}$ . The noiseless channel output symbol is shown next to branches. (c) Trellis section of an EPR4 channel (i.e., a PR channel with  $g(D) = 1 + D - D^2 - D^3$ ) when used with input alphabet  $\mathcal{X} = \{+1, -1\}$ . The noiseless channel output symbol is shown next to branches. (d) Trellis section of an FS-JSWTC comprised of a third-order FSMS, a dicode channel to Bob, and an EPR4 channel to Eve. State transition probabilities and noiseless channel output symbols (one noiseless channel output symbol for Bob's channel, one noiseless channel output symbol for Eve's channel) are shown next to branches.

where  $m_B$  and  $m_E$  are the degrees of  $g^B(D)$  and  $g^E(D)$ , respectively, the state space is given by  $\mathcal{S} \triangleq \mathcal{X}^\nu$  and the state at time  $t \in \mathbb{Z}$  is given by  $S_t \triangleq \mathbf{X}_{t-\nu+1}^t \in \mathcal{S}$ .

*Assumption 7.* In the following, we will focus on the case where  $\bar{\nu} \geq m_B$  and  $\bar{\nu} \geq m_E$ , which implies that  $\nu = \max(\bar{\nu}, m_B, m_E) = \bar{\nu}$ . With suitable notation, more general cases can be handled.  $\square$

Thanks to Assumption 7, the state transition probabilities of the finite-state machine modeling the FS-JSWTC will be the same as the state transition probabilities of the FSMS.

*Definition 8.* Let  $\mathcal{B}$  denote the set of all valid consecutive state pairs  $(s_{t-1}, s_t) \in \mathcal{S} \times \mathcal{S}$  for any  $t \in \mathbb{Z}$ . Moreover, let

$$\overrightarrow{\mathcal{S}}_i \triangleq \{j \mid (i, j) \in \mathcal{B}\}, \quad \overleftarrow{\mathcal{S}}_j \triangleq \{i \mid (i, j) \in \mathcal{B}\},$$

be the set of states  $S_t$  reachable from state  $S_{t-1} = i$  and the set of states  $S_{t-1}$  that can reach  $S_t = j$ , respectively.  $\square$

*Definition 9.* For  $(i, j) \in \mathcal{B}$ , let  $p_{ij}$  be the time-invariant probability of going from state

$S_{t-1} = i$  to state  $S_t = j$  for any  $t \in \mathbb{Z}$ . We assume that  $\{p_{ij}\}_{(i,j) \in \mathcal{B}}$  is such that the FSMS is ergodic, and so there is a unique stationary state probability distribution  $\{\mu_i\}_{i \in \mathcal{S}}$ , i.e.,  $p_{S_t}(i) = \mu_i$  for all  $t \in \mathbb{Z}$ . Finally, let  $\{Q_{ij}\}_{(i,j) \in \mathcal{B}}$  be defined by  $Q_{ij} \triangleq \mu_i \cdot p_{ij}$ ,  $(i, j) \in \mathcal{B}$ .

In the above definition, we started with  $\{p_{ij}\}_{(i,j) \in \mathcal{B}}$  and derived  $\{\mu_i\}_{i \in \mathcal{S}}$  and  $\{Q_{ij}\}_{(i,j) \in \mathcal{B}}$  from it. However, for analytical purposes, it turns out to be beneficial to start with  $\{Q_{ij}\}_{(i,j) \in \mathcal{B}}$  and derive  $\{p_{ij}\}_{(i,j) \in \mathcal{B}}$  and  $\{\mu_i\}_{i \in \mathcal{S}}$  from  $\{Q_{ij}\}_{(i,j) \in \mathcal{B}}$ . Note that the set of all  $\{Q_{ij}\}_{(i,j) \in \mathcal{B}}$  is given by the polytope  $\mathcal{Q}(\mathcal{B})$ , where

$$\mathcal{Q}(\mathcal{B}) \triangleq \left\{ \{Q_{ij}\}_{(i,j) \in \mathcal{B}} \mid Q_{ij} \geq 0, \forall (i, j) \in \mathcal{B}; \sum_{(i,j) \in \mathcal{B}} Q_{ij} = 1; \sum_{j \in \overrightarrow{\mathcal{S}}_i} Q_{ij} = \sum_{k \in \overleftarrow{\mathcal{S}}_i} Q_{ki}, \forall i \in \mathcal{S} \right\}.$$

(See [10] for similar observations.) In the following, we will use the short-hand notation  $\mathbf{Q}$  for  $\{Q_{ij}\}_{(i,j) \in \mathcal{B}}$ .

*Example 10.* Consider an FS-JSWTC

- where the FSMS is as in Remark 2 described by the triple  $(\mathcal{X}, \bar{\nu}, p_{X_t|X_{t-\bar{\nu}}^{t-1}}(x_t | \mathbf{x}_{t-\bar{\nu}}^{t-1}))$  with  $\mathcal{X} = \{+1, -1\}$  and  $\bar{\nu} = 3$  (see Fig. 1(a)),
- where Bob's channel is a dicode channel, i.e.,  $g^B(D) = 1 - D$  (see Fig. 1(b)), and
- where Eve's channel is an EPR4 channel, i.e.,  $g^E(D) = 1 + D - D^2 - D^3$  (see Fig. 1(c)).

This setup satisfies Assumption 7 and so  $\nu = \bar{\nu} = 3$ . All possible state sequences of an FS-JSWTC can be represented by a trellis diagram. Because of the assumed time-invariance, it is sufficient to show a single trellis section, as is done in Fig. 1(d) for the present example.

□

*Remark 11 (Parameterized family of  $\mathbf{Q}$ ).* Frequently, we will consider the setup where  $\mathbf{Q}(\theta)$  is a function of some parameter  $\theta$ . More precisely, for every  $(i, j) \in \mathcal{B}$ , we let  $Q_{ij}(\theta)$  be a smooth function of some parameter  $\theta$ , where  $\theta$  varies over a suitable range. We require that for every  $\theta$  it holds that  $\mathbf{Q}(\theta) = \{Q_{ij}(\theta)\}_{(i,j) \in \mathcal{B}} \in \mathcal{Q}(\mathcal{B})$ . For every,  $(i, j) \in \mathcal{B}$ , we denote the derivative of  $Q_{ij}(\theta)$  w.r.t.  $\theta$  and evaluated at  $\tilde{\theta}$  by  $Q_{ij}^\theta(\tilde{\theta})$ . We denote the corresponding steady-state and the transition probabilities parameterized by  $\theta$  by  $\mu_i(\theta)$  and  $p_{ij}(\theta)$ , respectively. Similarly, we denote their derivatives w.r.t.  $\theta$  and evaluated at  $\tilde{\theta}$  by  $\mu_i^\theta(\tilde{\theta})$  and  $p_{ij}^\theta(\tilde{\theta})$ , respectively.

Obviously, we have

$$\sum_{(i,j) \in \mathcal{B}} Q_{ij}^\theta(\tilde{\theta}) = 0, \quad \sum_{i \in \mathcal{S}} \mu_i^\theta(\tilde{\theta}) = 0. \quad (2)$$

□

*Remark 12.* Some technical remarks concerning the considered setup:

- It is well known that PR channels are indecomposable FSMCs [6], which means that the influence of the initial state vanishes over time, which implies that information rates are well defined even if the initial state is not known.
- Algorithm 1 in Section IV will make use of Perron–Frobenius theory for irreducible non-negative matrices. One can verify that the relevant matrix is indeed irreducible, except for uninteresting boundary cases.

□

### C. Achievable Secure Rates

In this section we summarize some known results for wiretap channels, along with establishing some achievable secure rates for PR-WTCs.

Information-spectrum methods have been used to analyze the fundamental limits of secure communication over arbitrary wiretap channels [18]. By adopting the notations in [18], the *spectral inf/sup-mutual information rates* are defined to be

$$\begin{aligned} \text{p-lim sup}_{n \rightarrow \infty} \frac{1}{n} i(\mathbf{X}_1^n; \mathbf{Y}_1^n) &\triangleq \inf \left\{ \alpha : \lim_{n \rightarrow \infty} \Pr \left( \frac{1}{n} i(\mathbf{X}_1^n; \mathbf{Y}_1^n) > \alpha \right) = 0 \right\}, \\ \text{p-lim inf}_{n \rightarrow \infty} \frac{1}{n} i(\mathbf{X}_1^n; \mathbf{Y}_1^n) &\triangleq \sup \left\{ \beta : \lim_{n \rightarrow \infty} \Pr \left( \frac{1}{n} i(\mathbf{X}_1^n; \mathbf{Y}_1^n) < \beta \right) = 0 \right\}, \end{aligned}$$

where p-lim is the probability limit operator.

*Lemma 13.* [17, Lemma 2] For an arbitrary wiretap channel  $(\mathcal{X}, \{p_{\mathbf{Y}_1^n, \mathbf{Z}_1^n | \mathbf{X}_1^n}(\mathbf{y}_1^n, \mathbf{z}_1^n | \mathbf{x}_1^n)\}_{n=1}^\infty, \mathcal{Y}, \mathcal{Z})$  consisting of an arbitrary input alphabet  $\mathcal{X}$ , two arbitrary output alphabets  $\mathcal{Y}$  and  $\mathcal{Z}$  corresponding to Bob's and Eve's observations, respectively, and a sequence of transition probabilities  $\{p_{\mathbf{Y}_1^n, \mathbf{Z}_1^n | \mathbf{X}_1^n}(\mathbf{y}_1^n, \mathbf{z}_1^n | \mathbf{x}_1^n)\}_{n=1}^\infty$ , all secure rates  $R_s$  satisfying

$$R_s < \max_{\{\mathbf{X}_1^n\}_{n=1}^\infty} \left( \text{p-lim inf}_{n \rightarrow \infty} \frac{1}{n} i(\mathbf{X}_1^n; \mathbf{Y}_1^n) - \text{p-lim sup}_{n \rightarrow \infty} \frac{1}{n} i(\mathbf{X}_1^n; \mathbf{Z}_1^n) \right)$$

are achievable under the reliability criterion

$$\limsup_{n \rightarrow \infty} \epsilon_n = 0, \quad (3)$$

and the secrecy criterion

$$\text{p-lim sup}_{n \rightarrow \infty} d_{\mathcal{M}_n \times \mathcal{Z}^n}(p_{M_n, \mathbf{Z}_1^n}, p_{M_n} p_{\mathbf{Z}_1^n}) = 0, \quad (4)$$

where  $\epsilon_n$  is the probability of error of Bob's decoder for a block code of length  $n$  and where  $M_n$  is the transmitted message uniformly chosen from an alphabet  $\mathcal{M}_n$ .

Note that the secrecy criterion (4) is stronger than the so-called *weak secrecy criterion*, which is defined as

$$\text{p-lim sup}_{n \rightarrow \infty} \frac{1}{n} I(M_n; \mathbf{X}_1^n) = 0,$$

and weaker than the so-called *strong secrecy criterion*, which is defined as

$$\text{p-lim sup}_{n \rightarrow \infty} I(M_n; \mathbf{X}_1^n) = 0,$$

see [18, Lemma 1].

Lemma 13 can be leveraged to deduce the following achievability result for PR-WTCs.

*Proposition 14.* Consider some PR-WTC described by the quadruple  $(g^B(D), g^E(D), \sigma_B^2, \sigma_E^2)$  and with input alphabet  $\mathcal{X}$ . For any integer  $\nu \geq \max(m_B, m_E)$ , any positive integer  $\ell$ , and any input distribution  $p_{\mathbf{X}_{-\nu+1}^\ell}$ , all secure rates  $R_s$  satisfying

$$R_s < \frac{1}{\ell + 2\nu} \left( I(\mathbf{X}_1^\ell; \mathbf{Y}_1^\ell | \mathbf{X}_{-\nu+1}^0) - I(\mathbf{X}_1^\ell; \mathbf{Z}_1^\ell | \mathbf{X}_{-\nu+1}^0) - 3\nu \cdot \log |\mathcal{X}| \right)$$

are achievable on this PR-WTC under the reliability criterion (3) and the secrecy criterion (4).

*Proof.* See Appendix A. □

*Definition 15.* Consider an FS-JSWTC as in Definition 6 with an FSMS described by  $\mathbf{Q}$ .

We define

$$R_s(\mathbf{Q}) \triangleq \lim_{n \rightarrow \infty} \frac{1}{n} \left( I(\mathbf{S}_1^n; \mathbf{Y}_1^n | S_0) - I(\mathbf{S}_1^n; \mathbf{Z}_1^n | S_0) \right). \quad (5)$$

□

*Corollary 16.* Consider an FS-JSWTC as in Definition 6 with an FSMS described by  $\mathbf{Q}$ . All secure rates  $R_s$  satisfying

$$R_s < R_s(\mathbf{Q})$$

are achievable under the reliability criterion (3) and the secrecy criterion (4).

*Proof.* Let  $\nu$  be the memory of the associated FS-JSWTC (see (1)). It is clear that  $I(\mathbf{X}_1^n; \mathbf{Y}_1^n | \mathbf{X}_{-\nu+1}^0) = I(\mathbf{S}_1^n; \mathbf{Y}_1^n | S_0)$  and  $I(\mathbf{X}_1^n; \mathbf{Z}_1^n | \mathbf{X}_{-\nu+1}^0) = I(\mathbf{S}_1^n; \mathbf{Z}_1^n | S_0)$ . Invoking Proposition 14 and letting  $n \rightarrow \infty$  proves the promised result. □

We are now in a position to introduce the notion of constrained secrecy capacity, which is a key quantity to be studied in the subsequent parts of this paper.

*Definition 17.* Consider an FS-JSWTC as in Definition 6, where the FSMS described by  $\mathbf{Q}$  can vary in  $\mathcal{Q}(\mathcal{B})$ . The constrained secrecy capacity (or, more precisely, the  $\mathcal{Q}(\mathcal{B})$ -constrained secrecy capacity) is defined as

$$C_{\mathcal{Q}(\mathcal{B})} \triangleq \max_{\mathbf{Q} \in \mathcal{Q}(\mathcal{B})} R_s(\mathbf{Q}).$$

### III. SECURE RATE: ESTIMATION

Throughout this section, we consider an FS-JSWTC as in Definition 6, where the FSMS is described by  $\mathbf{Q} \in \mathcal{Q}(\mathcal{B})$ . The secure rate in  $R_s(\mathbf{Q})$  can be efficiently estimated using variants of the algorithms in [24]. (We omit the details.) The main purpose of this section is to present an alternative approach for estimating  $R_s(\mathbf{Q})$ . Although the resulting algorithms by themselves are slightly less efficient than the estimation algorithms based on [24], they are based on quantities that need to be calculated as part of the optimization algorithm presented in the next section. Therefore, when running these optimization algorithms, these quantities are readily available and can be used to estimate  $R_s(\mathbf{Q})$ .

$$T_{ij}^B(\mathbf{Q}) \triangleq \lim_{n \rightarrow \infty} \frac{1}{n} \sum_{t=1}^n \sum_{\mathbf{y}_1^n \in \mathcal{Y}^n} p_{\mathbf{Y}_1^n}(\mathbf{y}_1^n) \cdot \log \left( \frac{p_{S_{t-1}, S_t | \mathbf{Y}_1^n}(i, j | \mathbf{y}_1^n)^{p_{S_{t-1}, S_t | \mathbf{Y}_1^n}(i, j | \mathbf{y}_1^n) / \mu_i p_{ij}}}{p_{S_{t-1} | \mathbf{Y}_1^n}(i | \mathbf{y}_1^n)^{p_{S_{t-1} | \mathbf{Y}_1^n}(i | \mathbf{y}_1^n) / \mu_i}} \right) \quad (4)$$

$$T_{ij}^E(\mathbf{Q}) \triangleq \lim_{n \rightarrow \infty} \frac{1}{n} \sum_{t=1}^n \sum_{\mathbf{z}_1^n \in \mathcal{Z}^n} p_{\mathbf{Z}_1^n}(\mathbf{z}_1^n) \cdot \log \left( \frac{p_{S_{t-1}, S_t | \mathbf{Z}_1^n}(i, j | \mathbf{z}_1^n)^{p_{S_{t-1}, S_t | \mathbf{Z}_1^n}(i, j | \mathbf{z}_1^n) / \mu_i p_{ij}}}{p_{S_{t-1} | \mathbf{Z}_1^n}(i | \mathbf{z}_1^n)^{p_{S_{t-1} | \mathbf{Z}_1^n}(i | \mathbf{z}_1^n) / \mu_i}} \right), \quad (5)$$

$$\check{T}_{ij}^B(\mathbf{Q}) \triangleq \frac{1}{n} \sum_{t=1}^n \log \left( \frac{p_{S_{t-1}, S_t | \mathbf{Y}_1^n}(i, j | \check{\mathbf{y}}_1^n)^{p_{S_{t-1}, S_t | \mathbf{Y}_1^n}(i, j | \check{\mathbf{y}}_1^n) / \mu_i p_{ij}}}{p_{S_{t-1} | \mathbf{Y}_1^n}(i | \check{\mathbf{y}}_1^n)^{p_{S_{t-1} | \mathbf{Y}_1^n}(i | \check{\mathbf{y}}_1^n) / \mu_i}} \right), \quad (6)$$

$$\check{T}_{ij}^E(\mathbf{Q}) \triangleq \frac{1}{n} \sum_{t=1}^n \log \left( \frac{p_{S_{t-1}, S_t | \mathbf{Z}_1^n}(i, j | \check{\mathbf{z}}_1^n)^{p_{S_{t-1}, S_t | \mathbf{Z}_1^n}(i, j | \check{\mathbf{z}}_1^n) / \mu_i p_{ij}}}{p_{S_{t-1} | \mathbf{Z}_1^n}(i | \check{\mathbf{z}}_1^n)^{p_{S_{t-1} | \mathbf{Z}_1^n}(i | \check{\mathbf{z}}_1^n) / \mu_i}} \right). \quad (7)$$

---

*Definition 18 ( $T_{ij}^B$  and  $T_{ij}^E$  values).* For every  $(i, j) \in \mathcal{B}$ , we define  $T_{ij}^B(\mathbf{Q})$  and  $T_{ij}^E(\mathbf{Q})$  to be, respectively, as shown in (4) and (5) at the top of the next page.  $\square$

The expressions in Definition 18 are similar to the expression for  $\check{T}_{ij}^{(N)}$  in [10, Lemma 70], part ‘‘second possibility.’’

*Proposition 19 (Secure information rate).* The secure rate of the FS-JSWTC under consideration can be expressed as follows in terms of the  $T_{ij}^B$  and  $T_{ij}^E$  values:

$$R_s(\mathbf{Q}) = \sum_{(i, j) \in \mathcal{B}} Q_{ij} \cdot (T_{ij}^B(\mathbf{Q}) - T_{ij}^E(\mathbf{Q})).$$

*Proof.* See Appendix B.  $\square$

*Remark 20.* The reformulation of  $R_s(\mathbf{Q})$  in Proposition 19 can be used to efficiently estimate  $R_s(\mathbf{Q})$  as follows:<sup>2</sup>

- 1) Generate a sequence  $\check{\mathbf{x}}_1^n$  based on the FSMS  $\mathbf{Q}$ .
- 2) Simulate Bob’s channel with  $\check{\mathbf{x}}_1^n$  at the input to obtain  $\check{\mathbf{y}}_1^n$  at the output.
- 3) Simulate Eve’s channel with  $\check{\mathbf{x}}_1^n$  at the input to obtain  $\check{\mathbf{z}}_1^n$  at the output.
- 4) For every  $(i, j) \in \mathcal{B}$ , compute (6) and (7) as shown at the top of the page. These quantities can be efficiently computed with the help of variants of the sum-product / BCJR algorithm. (See [10] for similar observations.)

<sup>2</sup>The accuracy of the approximation can be controlled by choosing  $n$  suitably large.

5) Estimate  $R_s(\mathbf{Q})$  by the quantity

$$\check{R}_s(\mathbf{Q}) = \sum_{(i,j) \in \mathcal{B}} Q_{ij} \cdot (\check{T}_{ij}^B(\mathbf{Q}) - \check{T}_{ij}^E(\mathbf{Q})).$$

□

#### IV. SECURE RATE: OPTIMIZATION

Throughout this section, we consider an FS-JSWTC as in Definition 6, where the FSMS described by  $\mathbf{Q}$  varies in  $\mathcal{Q}(\mathcal{B})$ . The optimization problem appearing in the specification of the constrained capacity  $C_{\mathcal{Q}(\mathcal{B})}$  in Definition 17 turns out to be difficult to solve because the function  $R_s(\mathbf{Q})$  is non-concave in general. Given this, we focus in this section on efficient algorithms for finding a local maximum of  $R_s(\mathbf{Q})$ . We do this by formulating an iterative algorithm inspired by the expectation-maximization (EM) algorithm. Namely, the presented algorithm is an algorithm that at every step approximates the function  $R_s(\mathbf{Q})$  by a suitable surrogate function that can be efficiently maximized. Related techniques were also used in [10], [25].

##### A. Outline of the Optimization Algorithm

The proposed algorithm is an iterative algorithm that works as follows:

- Assume that at the current iteration the algorithm has found the FSMS described by  $\tilde{\mathbf{Q}} \triangleq \{\tilde{Q}_{ij}\}_{(i,j) \in \mathcal{B}}$ .
- Around  $\mathbf{Q} = \tilde{\mathbf{Q}}$ , we approximate the function  $R_s(\mathbf{Q})$  over  $\mathcal{Q}(\mathcal{B})$  by the surrogate function  $\psi_{\tilde{\mathbf{Q}}}(\mathbf{Q})$  over  $\mathcal{Q}(\mathcal{B})$  satisfying the following properties:
  - The value of  $\psi_{\tilde{\mathbf{Q}}}(\mathbf{Q})$  matches the value of  $R_s(\mathbf{Q})$  at  $\mathbf{Q} = \tilde{\mathbf{Q}}$ .
  - The gradient of  $\psi_{\tilde{\mathbf{Q}}}(\mathbf{Q})$  w.r.t.  $\mathbf{Q}$  matches the gradient of  $R_s(\mathbf{Q})$  w.r.t.  $\mathbf{Q}$  at  $\mathbf{Q} = \tilde{\mathbf{Q}}$ .
  - The function  $\psi_{\tilde{\mathbf{Q}}}(\mathbf{Q})$  is concave in  $\mathbf{Q}$  and can be efficiently maximized.
- Replace  $\tilde{\mathbf{Q}}$  by the  $\mathbf{Q}$  maximizing  $\psi_{\tilde{\mathbf{Q}}}(\mathbf{Q})$ .

A sketch of these functions is shown in Fig. 2.

In the following, in the same way that we derived  $\{p_{ij}\}_{(i,j) \in \mathcal{B}}$  and  $\{\mu_i\}_{i \in \mathcal{S}}$  from  $\mathbf{Q} = \{Q_{ij}\}_{(i,j) \in \mathcal{B}}$ , we will derive  $\{\tilde{p}_{ij}\}_{(i,j) \in \mathcal{B}}$  and  $\{\tilde{\mu}_i\}_{i \in \mathcal{S}}$  from  $\tilde{\mathbf{Q}} = \{\tilde{Q}_{ij}\}_{(i,j) \in \mathcal{B}}$ .

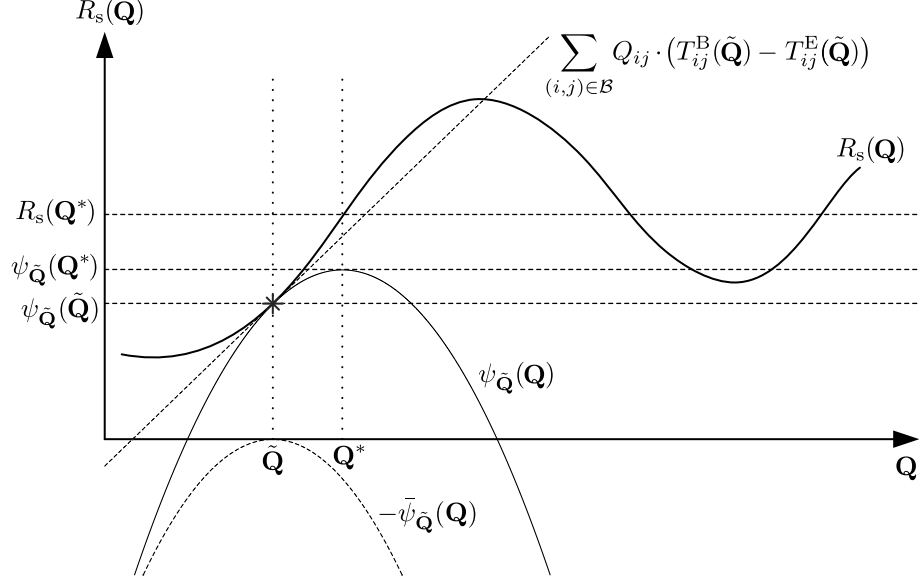


Fig. 2: Sketch of the functions appearing in the optimization algorithm discussed in Section IV.

### B. The Surrogate Function and its Properties

*Definition 21 (Surrogate function).* The surrogate function based on  $\tilde{\mathbf{Q}}$  is defined to be

$$\psi_{\tilde{\mathbf{Q}}}(\mathbf{Q}) \triangleq \sum_{(i,j) \in \mathcal{B}} Q_{ij} \cdot (T_{ij}^B(\tilde{\mathbf{Q}}) - T_{ij}^E(\tilde{\mathbf{Q}})) - \bar{\psi}_{\tilde{\mathbf{Q}}}(\mathbf{Q}), \quad (8)$$

where

$$\begin{aligned} \bar{\psi}_{\tilde{\mathbf{Q}}}(\mathbf{Q}) \triangleq \kappa' \cdot & \left( \sum_{(i,j) \in \mathcal{B}} \tilde{Q}_{ij} \cdot (1 + \kappa \cdot (\delta Q)_{ij}) \cdot \log(1 + \kappa \cdot (\delta Q)_{ij}) \right. \\ & \left. - \sum_{i \in \mathcal{S}} \tilde{\mu}_i \cdot (1 + \kappa \cdot (\delta \mu)_i) \cdot \log(1 + \kappa \cdot (\delta \mu)_i) \right). \end{aligned}$$

Here, for every  $(i, j) \in \mathcal{B}$ , the quantities  $(\delta Q)_{ij}$  and  $(\delta \mu)_i$  are defined to be, respectively,

$$(\delta Q)_{ij} \triangleq \frac{Q_{ij} - \tilde{Q}_{ij}}{\tilde{Q}_{ij}}, \quad (\delta \mu)_i \triangleq \frac{\mu_i - \tilde{\mu}_i}{\tilde{\mu}_i}.$$

Furthermore, the real parameters  $0 < \kappa \leq 1$  and  $\kappa' > 0$  are used to control the shape of  $\bar{\psi}_{\tilde{\mathbf{Q}}}(\mathbf{Q})$ , and with that the shape of  $\psi_{\tilde{\mathbf{Q}}}(\mathbf{Q})$ . (These parameters can be used to control the aggressiveness of the search step size.)  $\square$

*Assumption 22.* In order to show that the surrogate function  $\psi_{\tilde{\mathbf{Q}}}(\mathbf{Q})$  in Definition 21 has the promised properties, we consider a parameterization  $\mathbf{Q}(\theta)$  of  $\mathbf{Q}$  as discussed in Remark 11.

Beyond assuming that the parameterization is smooth and that there is a value  $\tilde{\theta}$  such that  $\tilde{\mathbf{Q}} = \mathbf{Q}(\tilde{\theta})$ , we make no assumption on this parameterization.  $\square$

In the following, we will use the short-hand notations  $R_s(\theta)$  and  $\psi_{\tilde{\mathbf{Q}}}(\theta)$  for  $R_s(\mathbf{Q}(\theta))$  and  $\psi_{\tilde{\mathbf{Q}}}(\mathbf{Q}(\theta))$ , respectively.

*Lemma 23 (Property 1 of the surrogate function  $\psi$ ).* The value of  $\psi_{\tilde{\mathbf{Q}}}(\mathbf{Q})$  matches the value of  $R_s(\mathbf{Q})$  at  $\mathbf{Q} = \tilde{\mathbf{Q}}$ , i.e.,

$$\psi_{\tilde{\mathbf{Q}}}(\tilde{\mathbf{Q}}) = R_s(\tilde{\mathbf{Q}}),$$

and, in terms of the parameterization defined above,

$$\psi_{\tilde{\mathbf{Q}}}(\tilde{\theta}) = R_s(\tilde{\theta}).$$

*Proof.* We start by noting that  $\mathbf{Q} = \tilde{\mathbf{Q}}$  implies that  $(\delta Q)_{ij} = 0$  and  $(\delta \mu)_i = 0$  for all  $(i, j) \in \mathcal{B}$ , which in turn implies that  $\bar{\psi}_{\tilde{\mathbf{Q}}}(\tilde{\mathbf{Q}}) = 0$ . The result  $\psi_{\tilde{\mathbf{Q}}}(\tilde{\mathbf{Q}}) = R_s(\tilde{\mathbf{Q}})$  follows then from the definition of  $\psi_{\tilde{\mathbf{Q}}}(\mathbf{Q})$  in Definition 21, along with Proposition 19.  $\square$

*Lemma 24 (Property 2 of the surrogate function  $\psi$ ).* The gradient of  $\psi_{\tilde{\mathbf{Q}}}(\mathbf{Q})$  w.r.t.  $\mathbf{Q}$  matches the gradient of  $R_s(\mathbf{Q})$  w.r.t.  $\mathbf{Q}$  at  $\mathbf{Q} = \tilde{\mathbf{Q}}$ , i.e.,

$$\frac{d}{d\theta} \psi_{\tilde{\mathbf{Q}}}(\theta) \Big|_{\theta=\tilde{\theta}} = \frac{d}{d\theta} R_s(\theta) \Big|_{\theta=\tilde{\theta}},$$

for any parameterization as defined above.

*Proof.* We start by showing that

$$\frac{d}{d\theta} \bar{\psi}_{\tilde{\mathbf{Q}}}(\theta) \Big|_{\theta=\tilde{\theta}} = 0. \quad (9)$$

Indeed,

$$\begin{aligned} \frac{d}{d\theta} \bar{\psi}_{\tilde{\mathbf{Q}}}(\theta) \Big|_{\theta=\tilde{\theta}} &= \kappa \kappa' \cdot \left( \sum_{(i,j) \in \mathcal{B}} Q_{ij}^\theta(\tilde{\theta}) \cdot \log(1 + \kappa \cdot (\delta Q(\tilde{\theta}))_{ij}) - \sum_{i \in \mathcal{S}} \mu_i^\theta(\tilde{\theta}) \cdot \log(1 + \kappa \cdot (\delta \mu(\tilde{\theta}))_i) \right) \Big|_{\theta=\tilde{\theta}} \\ &= 0. \end{aligned}$$

We then have

$$\begin{aligned} \frac{d}{d\theta} \psi_{\tilde{\mathbf{Q}}}(\theta) \Big|_{\theta=\tilde{\theta}} &= \frac{d}{d\theta} (\psi_{\tilde{\mathbf{Q}}}(\theta) + \bar{\psi}_{\tilde{\mathbf{Q}}}(\theta)) \Big|_{\theta=\tilde{\theta}} = \frac{d}{d\theta} \left( \sum_{(i,j) \in \mathcal{B}} Q_{ij}(\theta) \cdot (T_{ij}^B(\tilde{\theta}) - T_{ij}^E(\tilde{\theta})) \right) \Big|_{\theta=\tilde{\theta}} \\ &= \frac{d}{d\theta} \left( \sum_{(i,j) \in \mathcal{B}} Q_{ij}(\theta) \cdot (T_{ij}^B(\theta) - T_{ij}^E(\theta)) \right) \Big|_{\theta=\tilde{\theta}} = \frac{d}{d\theta} R_s(\theta) \Big|_{\theta=\tilde{\theta}}, \end{aligned}$$

where the first equality follows from (9), where the second equality from Definition 21, where the third equality follows from [10, Lemma 64], and where the fourth equality follows from Proposition 19.  $\square$

*Remark 25.* Despite the close similarity between the third and fourth expression in the final display equation of the above proof, this is a non-trivial result because of the non-triviality of [10, Lemma 64].

*Lemma 26 (Convexity of the function  $\bar{\psi}_{\tilde{\mathbf{Q}}}(\mathbf{Q})$ ).* The function  $\bar{\psi}_{\tilde{\mathbf{Q}}}(\mathbf{Q})$  is convex over  $\mathbf{Q} \in \mathcal{Q}(\mathcal{B})$ .

*Proof.* See Appendix C.  $\square$

*Lemma 27 (Concavity of the surrogate function  $\psi_{\tilde{\mathbf{Q}}}(\mathbf{Q})$ ).* The surrogate function  $\psi_{\tilde{\mathbf{Q}}}(\mathbf{Q})$  is concave over  $\mathbf{Q} \in \mathcal{Q}(\mathcal{B})$ .

*Proof.* This follows immediately from Lemma 26 and from  $\sum_{(i,j) \in \mathcal{B}} Q_{ij} \cdot (T_{ij}^B(\tilde{\mathbf{Q}}) - T_{ij}^E(\tilde{\mathbf{Q}}))$  being a linear function of  $\mathbf{Q}$ .  $\square$

### C. Maximizing the Surrogate Function

Let  $\tilde{\mathbf{Q}}$  denote the FSMS distribution attained at the current iteration of the proposed algorithm. For the next iteration,  $\tilde{\mathbf{Q}}$  is replaced by  $\mathbf{Q}^* = \{Q_{ij}^*\}_{(i,j) \in \mathcal{B}}$ , where

$$\mathbf{Q}^* \triangleq \arg \max_{\mathbf{Q} \in \mathcal{Q}(\mathcal{B})} \psi_{\tilde{\mathbf{Q}}}(\mathbf{Q}). \quad (10)$$

In the following, in the same way that we derived  $\{p_{ij}\}_{(i,j) \in \mathcal{B}}$  and  $\{\mu_i\}_{i \in \mathcal{S}}$  from  $\mathbf{Q} = \{Q_{ij}\}_{(i,j) \in \mathcal{B}}$ , we will derive  $\{\tilde{p}_{ij}\}_{(i,j) \in \mathcal{B}}$  and  $\{\tilde{\mu}_i\}_{i \in \mathcal{S}}$  from  $\tilde{\mathbf{Q}} = \{\tilde{Q}_{ij}\}_{(i,j) \in \mathcal{B}}$  and  $\{p_{ij}^*\}_{(i,j) \in \mathcal{B}}$  and  $\{\mu_i^*\}_{i \in \mathcal{S}}$  from  $\mathbf{Q}^* = \{Q_{ij}^*\}_{(i,j) \in \mathcal{B}}$ .

*Proposition 28 (The optimum distribution  $\mathbf{Q}^*$ ).* The FSMS  $\mathbf{Q}^* = \{Q_{ij}^*\}_{(i,j) \in \mathcal{B}}$  in (10) can be found as follows.

- Let  $\mathbf{A} \triangleq (A_{ij})_{i,j \in \mathcal{S}}$  be the matrix with entries

$$A_{ij} \triangleq \begin{cases} \tilde{p}_{ij} \cdot \exp\left(\frac{\tilde{T}_{ij}^B - \tilde{T}_{ij}^E}{\kappa\kappa'}\right) & ((i, j) \in \mathcal{B}) \\ 0 & (\text{otherwise}) \end{cases}, \quad (11)$$

where  $\tilde{T}_{ij}^B \triangleq T_{ij}^B(\tilde{\mathbf{Q}})$  and  $\tilde{T}_{ij}^E \triangleq T_{ij}^E(\tilde{\mathbf{Q}})$  are defined according to Definition 18. Note that  $\mathbf{A}$  is a non-negative matrix, i.e., a matrix with non-negative entries.

- Let  $\rho$  be the Perron–Frobenius eigenvalue of the matrix  $\mathbf{A}$ , with corresponding right eigenvector  $\boldsymbol{\gamma} = (\gamma_j)_{j \in \mathcal{S}}$ .<sup>3</sup>
- Define

$$\hat{p}_{ij}^* \triangleq \frac{A_{ij}}{\rho} \cdot \frac{\gamma_j}{\gamma_i}, \quad (i, j) \in \mathcal{B}. \quad (12)$$

- If

$$\kappa \geq \frac{\tilde{Q}_{ij} - \hat{Q}_{ij}^*}{\tilde{Q}_{ij}}, \quad (i, j) \in \mathcal{B}, \quad (13)$$

then the FSMS  $\mathbf{Q}^*$  is given by solving the system of linear equations

$$\begin{cases} Q_{ij}^* - \hat{p}_{ij}^* \sum_{j' \in \mathcal{S}_i} Q_{ij'}^* = \frac{1-\kappa}{\kappa} \cdot (\tilde{\mu}_i \hat{p}_{ij}^* - \tilde{Q}_{ij}), & (i, j) \in \mathcal{B}, \\ \sum_{r \in \mathcal{S}_i} Q_{ri}^* - \sum_{j \in \mathcal{S}_i} Q_{ij}^* = 0, & i \in \mathcal{S}, \\ \sum_{(i,j) \in \mathcal{B}} Q_{ij}^* = 1. \end{cases} \quad (14)$$

for  $\{Q_{ij}^*\}_{(i,j) \in \mathcal{B}}$ .

*Proof.* See Appendix D.  $\square$

*Remark 29.* Increasing the parameters  $\kappa$  and  $\kappa'$  has the effect of making the surrogate function narrower and steeper, implying a decreased step size.

*Remark 30.* A procedure similar to the procedure in Remark 20 can be used to efficiently find an approximation  $\check{\mathbf{Q}}^*$  to  $\mathbf{Q}^*$ :<sup>4</sup>

<sup>3</sup>Recall that the Perron–Frobenius eigenvalue of a irreducible non-negative matrix is the eigenvalue with largest absolute value. One can show that the Perron–Frobenius eigenvalue is a positive real number and that the corresponding right eigenvector can be multiplied by a suitable scalar such that all entries are positive real numbers.

<sup>4</sup>The accuracy of the approximation can be controlled by choosing  $n$  suitably large.

---

**Algorithm 1** Secure Rate Optimization

---

**Input:**

$n$   $\triangleright$  length of simulated codeword;  
 $\mathcal{B}$   $\triangleright$  set of all valid transition probabilities;  
 $\mathbf{Q}^{(0)} = (Q_{ij}^{(0)})$ :  $Q_{ij}^{(0)} \in \mathcal{Q}(\mathcal{B})$   $\triangleright$  initial point satisfying  $Q_{ij}^{(0)} > 0$  for all  $(i, j) \in \mathcal{B}$ ;  
 PR-WTC  $(g^B(D), g^E(D), \sigma_B^2, \sigma_E^2)$ ;  
 $\kappa$ :  $0 < \kappa \leq 1$   $\triangleright$  step size controlling parameter;  
 $\kappa'$ :  $\kappa' > 0$ ;  $\triangleright$  step size controlling parameter;

□ *Initialization:*

set  $r \leftarrow 0$ ;

▷ *Iteration* (until convergence)

2: Apply the procedure in Remark 30 with input  $\mathbf{Q} = \mathbf{Q}^{(r)}$  and output  $\check{\mathbf{Q}}$   
 (suitably change the parameters  $\kappa, \kappa'$  if necessary);

$\mathbf{Q}^{(r)} \leftarrow \check{\mathbf{Q}}$ ;

$r \leftarrow r + 1$ ;

◁ *End*

4: Use the procedure in Remark 20 with input  $\mathbf{Q} = \mathbf{Q}^{(r)}$  and output  $\check{R}_s$ ;  
**return**  $\check{R}_s$ .

---

- 1) Generate a sequence  $\check{\mathbf{x}}_1^n$  based on the FSMS  $\mathbf{Q} = \check{\mathbf{Q}}$ .
- 2) Simulate Bob's channel with  $\check{\mathbf{x}}_1^n$  at the input to obtain  $\check{\mathbf{y}}_1^n$  at the output.
- 3) Simulate Eve's channel with  $\check{\mathbf{x}}_1^n$  at the input to obtain  $\check{\mathbf{z}}_1^n$  at the output.
- 4) For every  $(i, j) \in \mathcal{B}$ , compute  $\check{T}_{ij}^B$  and  $\check{T}_{ij}^E$  according to (6) and (7) based on  $\mathbf{Q} = \check{\mathbf{Q}}$ .

These quantities can be efficiently computed with the help of variants of the sum-product / BCJR algorithm. (See [10] for similar observations.)

- 5) Let  $\check{\mathbf{A}} \triangleq (\check{A}_{ij})_{i,j \in \mathcal{S}}$  be the matrix with entries

$$\check{A}_{ij} \triangleq \begin{cases} \tilde{p}_{ij} \cdot \exp\left(\frac{\check{T}_{ij}^B - \check{T}_{ij}^E}{\kappa\kappa'}\right) & ((i, j) \in \mathcal{B}) \\ 0 & (\text{otherwise}) \end{cases}.$$

- 6) Find the Perron–Frobenius eigenvalue  $\check{\rho}$  and the corresponding right eigenvector  $\check{\gamma}$  of the matrix  $\check{\mathbf{A}}$ .
- 7) Compute

$$\check{p}_{ij}^* \triangleq \frac{\check{A}_{ij}}{\check{\rho}} \cdot \frac{\check{\gamma}_j}{\check{\gamma}_i}, \quad (i, j) \in \mathcal{B}.$$

8) Solve the system of linear equations

$$\left\{ \begin{array}{l} \check{Q}_{ij}^* - \check{p}_{ij}^* \sum_{j' \in \mathcal{S}_i} \check{Q}_{ij'}^* = \frac{1-\kappa}{\kappa} \cdot (\tilde{\mu}_i \check{p}_{ij}^* - \tilde{Q}_{ij}), \quad (i, j) \in \mathcal{B}, \\ \sum_{r \in \mathcal{S}_i} \check{Q}_{ri}^* - \sum_{j \in \mathcal{S}_i} \check{Q}_{ij}^* = 0, \quad i \in \mathcal{S}, \\ \sum_{(i,j) \in \mathcal{B}} \check{Q}_{ij}^* = 1. \end{array} \right.$$

for  $\{\check{Q}_{ij}^*\}_{(i,j) \in \mathcal{B}}$ .

9) Check if  $\check{Q}_{ij}^* \geq 0$ ,  $(i, j) \in \mathcal{B}$ . If not, reject the obtained solution, suitably change the parameters  $\kappa$  and  $\kappa'$ , and reapply this procedure.<sup>5</sup>

The complete algorithm for the proposed optimization method is summarized as Algorithm 1.

*Remark 31 (The EM Viewpoint).* The proposed algorithm can be considered as a variation of the well-known EM algorithm [26] comprised of two steps: Expectation (E-step) and Maximization (M-step). Namely, identifying a concave surrogate function of the secure rate function around a local operating point resembles the E-step and maximization of the surrogate function to achieve a higher secure rate corresponds to the M-step. With this, the proposed algorithm has similar convergence guarantees (to a local maximum of the secure rate function) as the EM algorithm [27].

## V. SIMULATION RESULTS AND DISCUSSION

In this section we apply the proposed algorithm, Algorithm 1, to two different PR-WTCs and study the obtained achievable secure rates.

In previous sections, in order to keep the notation simple, we used the channel input alphabet  $\mathcal{X} = \{+1, -1\}$  and unnormalized PR channel transfer polynomials. However, in this section we use the channel input alphabet  $\mathcal{X} = \{+\sqrt{E_s}, -\sqrt{E_s}\}$  and normalized PR channel transfer polynomials, where a normalized transfer polynomial  $g(D) \triangleq \sum_{t=0}^m g_t D^t \in \mathbb{R}[D]$  has to satisfy  $\sum_{t=0}^m |g_t|^2 = 1$ . (For a discussion on normalization of transfer polynomials, see, e.g., [28].)

<sup>5</sup>Alternatively, one could determine  $\{\check{Q}_{ij}^*\}_{(i,j) \in \mathcal{B}}$  based on  $\check{p}_{ij}^*$  and then verify if  $\kappa \geq (\tilde{Q}_{ij} - \check{Q}_{ij}^*)/\tilde{Q}_{ij}$ ,  $(i, j) \in \mathcal{B}$ . However, the proposed checks are obviously simpler to evaluate.

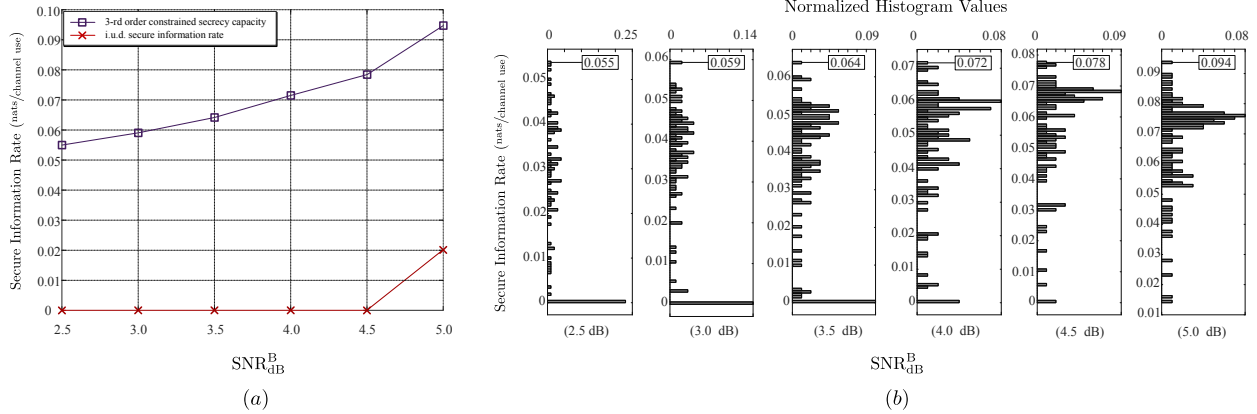


Fig. 3: Simulation results for the setup in Example 32. (a) The 3rd order constrained secrecy capacity and the secure rates of an i.u.d. input process when  $\text{SNR}_{\text{dB}}^{\text{E}} = 5.0$  dB. (b) Normalized histogram functions of the locally-optimum secure rates obtained from running Algorithm 1 with 100 different initializations.

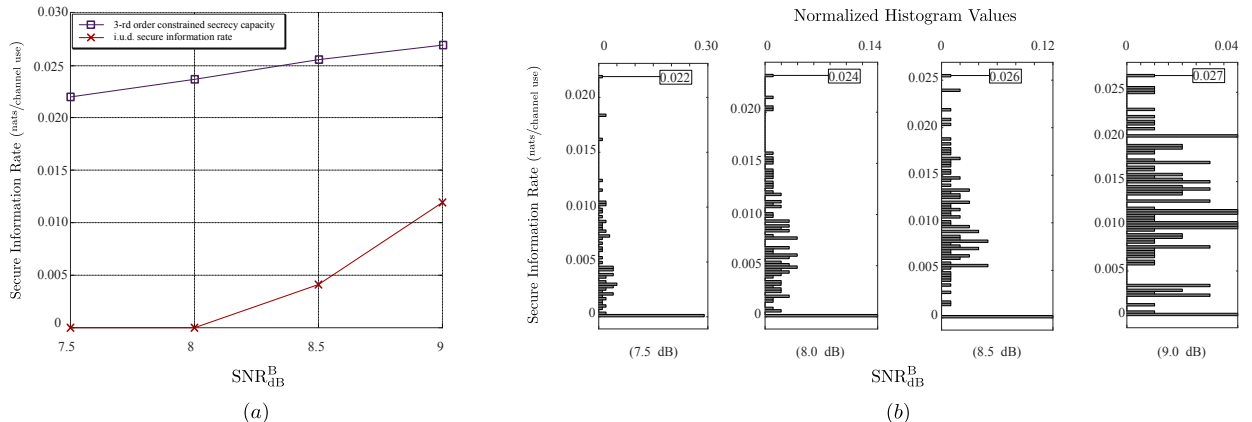


Fig. 4: Simulation results for the setup in Example 33. (a) The 3rd order constrained secrecy capacity and the secure rates of an i.u.d. input process when  $\text{SNR}_{\text{dB}}^{\text{E}} = 8.0$  dB. (b) Normalized histogram functions of the locally-optimum secure rates obtained from running Algorithm 1 with 100 different initializations.

### A. Simulation Results

In general, we consider the following PR-WTC setup:

- The transmitted symbols are BPSK modulated with the alphabet  $\mathcal{X} = \{+\sqrt{E_s}, -\sqrt{E_s}\}$ .
- Bob's channel is a PR channel with normalized transfer polynomial  $g^{\text{B}}(D)$  and additive white Gaussian noise of variance  $\sigma_{\text{B}}^2$ .
- Eve's channel is a PR channel with normalized transfer polynomial  $g^{\text{E}}(D)$  and additive white Gaussian noise of variance  $\sigma_{\text{E}}^2$ .
- The SNR of Bob's and Eve's channel is defined as  $\text{SNR}^{\text{B}} \triangleq E_s/\sigma_{\text{B}}^2$  and  $\text{SNR}^{\text{E}} \triangleq E_s/\sigma_{\text{E}}^2$ , which in terms of decibels are  $\text{SNR}_{\text{dB}}^{\text{B}} \triangleq 10 \log_{10}(E_s/\sigma_{\text{B}}^2)$  and  $\text{SNR}_{\text{dB}}^{\text{E}} \triangleq 10 \log_{10}(E_s/\sigma_{\text{E}}^2)$ ,

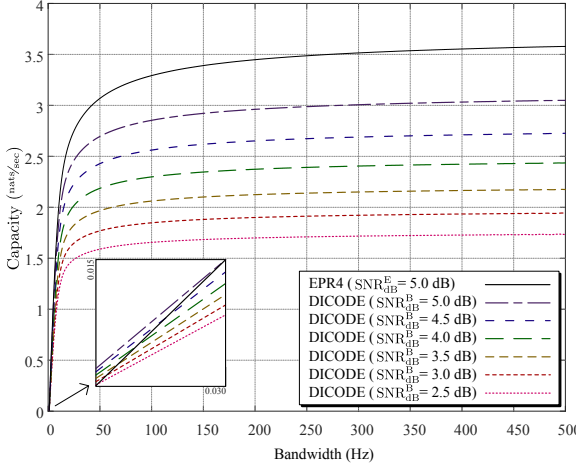


Fig. 5: Capacity of the dicode and the EPR4 channels in nats/sec with input power  $E_s = 1$  J, for the SNR values corresponding to Example 32.

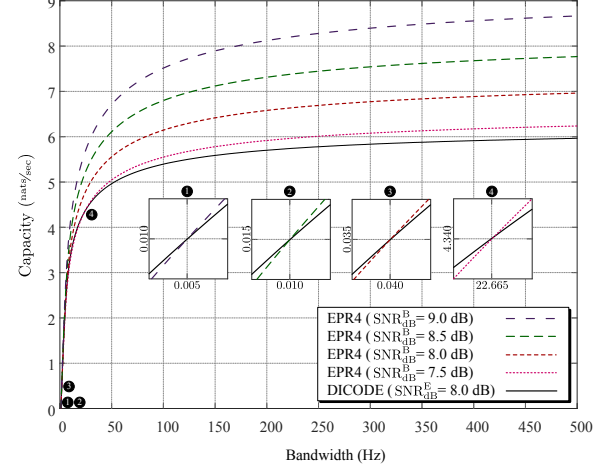


Fig. 6: Capacity of the dicode and the EPR4 channels in nats/sec with input power  $E_s = 1$  J, for the SNR values corresponding to Example 33.

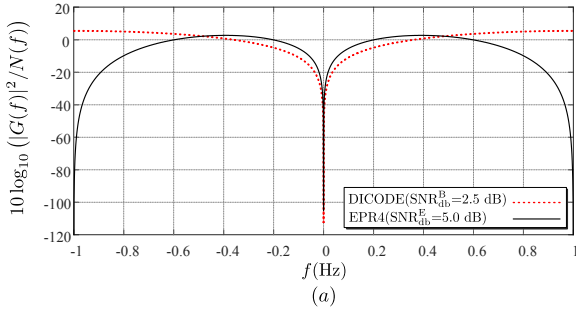


Fig. 7: The channel's gain-to-noise spectrum ratio in decibels per frequency (Hz) corresponding to Examples 32 and 33.

respectively.<sup>6</sup>

*Example 32.* We consider the following setup:

- An FSMS as in Remark 2 with  $\bar{\nu} = 3$ .
- Bob's channel is a dicode channel, i.e.,

$$g^B(D) = \frac{1}{\sqrt{2}} \cdot (1 - D).$$

- Eve's channel is an EPR4 channel, i.e.,

$$g^E(D) = \frac{1}{2} \cdot (1 + D - D^2 - D^3).$$

<sup>6</sup>If desired, these SNR values can be re-expressed in terms of  $E_s/N_0$  values, where  $N_0$  is the two-sided power spectral density of the AWGN process:  $E_s/N_0 = \frac{1}{2} \cdot (E_s/\sigma^2)$ .

Fig. 3(a) shows the obtained secure information rates: on the one hand for an *unoptimized* FSMS, i.e., an FSMS producing i.u.d. symbols, and, on the other hand, for an *optimized* FSMS, where the optimization was done with the help of Algorithm 1. In this plot, for every  $\text{SNR}_{\text{dB}}^{\text{B}}$  value, the best obtained secure information rate is plotted after running Algorithm 1 for 100 different initializations.<sup>7</sup> In fact, it is important to run Algorithm 1 with several initializations because the secure information rate is a highly fluctuating function, which is witnessed by the broad histograms in Fig. 3(b) that show the obtained secure information rates for various initializations of Algorithm 1.

*Example 33.* We consider the following setup:

- An FSMS as in Remark 2 with  $\bar{\nu} = 3$ .
- Bob's channel is an EPR4 channel, i.e.,

$$g^{\text{B}}(D) = \frac{1}{2} \cdot (1 + D - D^2 - D^3).$$

- Eve's channel is a dicode channel, i.e.,

$$g^{\text{E}}(D) = \frac{1}{\sqrt{2}} \cdot (1 - D).$$

The obtained results are shown in Figs. 4(a) and (b). (These figures are similar to Figs. 3(a) and (b) for Example 32.)

Note that when running Algorithm 1, we used  $\kappa$  and  $\kappa'$  values in the ranges  $0.8 \leq \kappa \leq 1$  and  $5 \leq \kappa' \leq 10$ , respectively. Typically, 30 to 40 iterations were needed to reach numerical convergence.

### B. Discussion

As we have seen in Section V-A, positive secure information rates are possible and optimizing the FSMS clearly benefits these rates. Interestingly, positive secure information rates are also possible when the point-to-point channel to Eve is “better” than the point-to-point channel to Bob. In order to make this discussion more insightful and analytically tractable, we consider in this section the scenario where the only channel input constraint is

<sup>7</sup>These initializations were generated with the help of Weyl's  $|\mathcal{S}|$ -dimensional equi-distributed sequences [29].

an average energy constraint. This allows us to use Fourier transform techniques and well-known “water-pouring” formulas for analyzing capacities of such point-to-point channels.

Namely, consider a PR channel described by the transfer polynomial  $g(D) = \sum_{t=0}^m g_t D^t$  and with additive (possibly non-white) Gaussian noise. The unconstrained (besides some average-energy constraint) capacity of this channel is given by the “water-pouring” formula (see, e.g., [28])

$$C = \frac{1}{2} \cdot \int_{-\infty}^{\infty} \max \left\{ 0, \log \left( \frac{\alpha}{N(f)/|G(f)|^2} \right) \right\} df,$$

where

$$G(f) = \begin{cases} \frac{\sum_{\ell=0}^m g_{\ell} e^{-j2\ell\pi fT}}{\sum_{\ell=0}^m |g_{\ell}|^2} & \text{(if } |f| \leq W) \\ 0 & \text{(otherwise)} \end{cases},$$

and where  $\alpha > 0$  is chosen such that

$$E_s = \int_{-\infty}^{\infty} \max \left\{ 0, \alpha - \frac{N(f)}{|G(f)|^2} \right\} df.$$

This capacity formula is based on the following assumptions:

- average energy constraint per input symbol  $E_s$ ;
- symbol period  $T$  (in seconds);
- a perfect lowpass filter of bandwidth  $W \triangleq \frac{1}{2T}$  and sampling at the Nyquist frequency  $1/T$  at the receiver side;
- power spectral density  $N(f)$  (in Watts per Hertz) of the additive Gaussian noise before the lowpass filter.

The resulting unconstrained capacities for a dicode and an EPR4 channel are shown in Fig. 5 and Fig. 6.

*Example 34* (Continuation of Example 32). Consider the scenario where  $E_s = 1 \text{ J}$ ,  $2.5 \text{ dB} \leq \text{SNR}_{\text{dB}}^B \leq 5 \text{ dB}$ , and  $\text{SNR}_{\text{dB}}^E = 5 \text{ dB}$ . It can be seen from Fig. 5 that Eve’s channel has a higher unconstrained capacity than Bob’s channel for sufficiently large enough bandwidth. In this sense, Bob’s channel is “worse” than Eve’s channel. However, luckily for Bob, there are frequencies where Bob’s channel has a better gain-to-noise spectrum ratio than Eve’s

channel, as can be seen from Fig. 7(a). This can be exploited by a suitably tuned source at the channel input toward obtaining positive secure information rates.

*Example 35* (Continuation of Example 33). Consider the scenario where  $E_s = 1 \text{ J}$ ,  $7.5 \text{ dB} \leq \text{SNR}_{\text{dB}}^B \leq 9 \text{ dB}$ , and  $\text{SNR}_{\text{dB}}^E = 8 \text{ dB}$ . It can be seen from Fig. 6 that Bob's channel has a higher unconstrained capacity than Eve's channel for sufficiently large enough bandwidth. In this sense, it is not unexpected that positive secure information rates are possible. Nevertheless, it is worthwhile to point out that here secure information rates are possible even though Bob's channel has larger memory and, for some selections of  $\text{SNR}_{\text{dB}}^B$ , higher noise power than Eve's channel (see Fig. 7(b)).

In a conventional DM-WTC [15], [16], Eve's channel necessarily has to be noisier than Bob's channel in order to achieve a positive secrecy capacity. This results in the capacity of Eve's channel to be less than the capacity of Bob's channel. In contrast, we showed that positive secure information rates are achievable on the PR-WTCs, even if

- the unconstrained capacity of Bob's channel is smaller than the unconstrained capacity of Eve's channel (Example 32);
- Bob's channel tolerates both a higher noise power and a larger memory compared with Eve's channel (Example 33).

## VI. CONCLUSION

In this paper, we have optimized an FSMS at the input of a PR-WTC toward (locally) maximizing the secrecy rate. Because directly maximizing the secrecy rate function is challenging, we have iteratively approximated the secrecy rate function by a surrogate function whose maximum can be found efficiently.

Our numerical results show that, by implicitly using the discrepancies between the frequency responses of Bob's and Eve's channels, it is possible to achieve positive secrecy rates also for setups where the unconstrained capacity of Eve's channel is larger than the unconstrained capacity of Bob's channel.

APPENDIX A  
PROOF OF PROPOSITION 14

Let  $\left\{\mathbf{X}_{k(\ell+2\nu)-\nu+1}^{k(\ell+2\nu)+(\ell+\nu)}\right\}_{k=-\infty}^{+\infty}$  be a block i.i.d. process where each block has length  $\ell + 2\nu$ . It suffices to specify the distribution of a single block  $\mathbf{X}_{k(\ell+2\nu)-\nu+1}^{k(\ell+2\nu)+(\ell+\nu)}$ . We set

$$X_{k(\ell+2\nu)+(\ell+1)} \triangleq 0, \quad \dots, \quad X_{k(\ell+2\nu)+(\ell+\nu)} \triangleq 0,$$

in order to ensure that there is no interference across blocks, while allowing  $\mathbf{X}_{k(\ell+2\nu)-\nu+1}^{k(\ell+2\nu)+\ell}$  to be arbitrarily distributed. It is easy to verify that

$$\left\{\mathbf{X}_{k(\ell+2\nu)-\nu+1}^{k(\ell+2\nu)+(\ell+\nu)}, \mathbf{Y}_{k(\ell+2\nu)-\nu+1}^{k(\ell+2\nu)+(\ell+\nu)}\right\}_{k=-\infty}^{+\infty},$$

is a joint block i.i.d. process. Similarly,

$$\left\{\mathbf{X}_{k(\ell+2\nu)-\nu+1}^{k(\ell+2\nu)+(\ell+\nu)}, \mathbf{Z}_{k(\ell+2\nu)-\nu+1}^{k(\ell+2\nu)+(\ell+\nu)}\right\}_{k=-\infty}^{+\infty},$$

is also a joint block i.i.d. process. It follows by the strong law of large numbers that

$$\begin{aligned} \lim_{n \rightarrow \infty} \frac{1}{n} i(\mathbf{X}_1^n; \mathbf{Y}_1^n) &= \frac{1}{\ell + 2\nu} I(\mathbf{X}_{-\nu+1}^{\ell+\nu}; \mathbf{Y}_{-\nu+1}^{\ell+\nu}) \quad \text{w.p. 1,} \\ \lim_{n \rightarrow \infty} \frac{1}{n} i(\mathbf{X}_1^n; \mathbf{Z}_1^n) &= \frac{1}{\ell + 2\nu} I(\mathbf{X}_{-\nu+1}^{\ell+\nu}; \mathbf{Z}_{-\nu+1}^{\ell+\nu}) \quad \text{w.p. 1.} \end{aligned}$$

Note that

$$\begin{aligned} I(\mathbf{X}_{-\nu+1}^{\ell+\nu}; \mathbf{Y}_{-\nu+1}^{\ell+\nu}) &\geq I(\mathbf{X}_{-\nu+1}^{\ell}; \mathbf{Y}_1^{\ell}) \\ &= I(\mathbf{X}_{-\nu+1}^0; \mathbf{Y}_1^{\ell}) + I(\mathbf{X}_1^{\ell}; \mathbf{Y}_1^{\ell} | \mathbf{X}_{-\nu+1}^0) \\ &\geq I(\mathbf{X}_1^{\ell}; \mathbf{Y}_1^{\ell} | \mathbf{X}_{-\nu+1}^0). \end{aligned}$$

Moreover,

$$\begin{aligned} I(\mathbf{X}_{-\nu+1}^{\ell+\nu}; \mathbf{Z}_{-\nu+1}^{\ell+\nu}) &= I(\mathbf{X}_{-\nu+1}^{\ell}; \mathbf{Z}_{-\nu+1}^{\ell+\nu}) \\ &= I(\mathbf{X}_{-\nu+1}^{\ell}; \mathbf{Z}_1^{\ell}) + I(\mathbf{X}_{-\nu+1}^{\ell}; \mathbf{Z}_{-\nu+1}^0 | \mathbf{Z}_1^{\ell}) + I(\mathbf{X}_{-\nu+1}^{\ell}; \mathbf{Z}_{\ell+1}^{\ell+\nu} | \mathbf{Z}_{-\nu+1}^{\ell}) \\ &= I(\mathbf{X}_1^{\ell}; \mathbf{Z}_1^{\ell} | \mathbf{X}_{-\nu+1}^0) + I(\mathbf{X}_{-\nu+1}^0; \mathbf{Z}_1^{\ell}) + I(\mathbf{X}_{-\nu+1}^{\ell}; \mathbf{Z}_{-\nu+1}^0 | \mathbf{Z}_1^{\ell}) + I(\mathbf{X}_{-\nu+1}^{\ell}; \mathbf{Z}_{\ell+1}^{\ell+\nu} | \mathbf{Z}_{-\nu+1}^{\ell}) \\ &= I(\mathbf{X}_1^{\ell}; \mathbf{Z}_1^{\ell} | \mathbf{X}_{-\nu+1}^0) + I(\mathbf{X}_{-\nu+1}^0; \mathbf{Z}_1^{\ell}) + I(\mathbf{X}_{-\nu+1}^0; \mathbf{Z}_{-\nu+1}^0 | \mathbf{Z}_1^{\ell}) + I(\mathbf{X}_{\ell-\nu+1}^{\ell}; \mathbf{Z}_{\ell+1}^{\ell+\nu} | \mathbf{Z}_{-\nu+1}^{\ell}) \\ &\leq I(\mathbf{X}_1^{\ell}; \mathbf{Z}_1^{\ell} | \mathbf{X}_{-\nu+1}^0) + 3\nu \log |\mathcal{X}|. \end{aligned}$$

Combining Lemma 13 with the above lower and upper bounds concludes the proof.

## APPENDIX B PROOF OF PROPOSITION 19

Reformulating the expression in (5), we obtain

$$\begin{aligned}
R_s &= \lim_{n \rightarrow \infty} \frac{1}{n} \left( I(\mathbf{S}_1^n; \mathbf{Y}_1^n | S_0) - I(\mathbf{S}_1^n; \mathbf{Z}_1^n | S_0) \right) &= \lim_{n \rightarrow \infty} \frac{1}{n} \sum_{t=1}^n \left( I(S_t; \mathbf{Y}_1^n | \mathbf{S}_0^{t-1}) - I(S_t; \mathbf{Z}_1^n | \mathbf{S}_0^{t-1}) \right) \\
&= \lim_{n \rightarrow \infty} \frac{1}{n} \sum_{t=1}^n \left( I(S_t; \mathbf{Y}_1^n | S_{t-1}) - I(S_t; \mathbf{Z}_1^n | S_{t-1}) \right) &= \lim_{n \rightarrow \infty} \frac{1}{n} \sum_{t=1}^n \left( H(S_t | \mathbf{Z}_1^n, S_{t-1}) - H(S_t | \mathbf{Y}_1^n, S_{t-1}) \right) \\
&= \sum_{(i,j) \in \mathcal{B}} Q_{ij} \cdot \left( T_{ij}^B(\mathbf{Q}) - T_{ij}^E(\mathbf{Q}) \right),
\end{aligned}$$

where the last equality is based on expressing  $H(S_t | \mathbf{Y}_1^n, S_{t-1})$  as

$$\begin{aligned}
H(S_t | \mathbf{Y}_1^n, S_{t-1}) &= - \sum_{(i,j) \in \mathcal{B}} \sum_{\mathbf{y}_1^n \in \mathcal{Y}^n} p_{S_t, S_{t-1}, \mathbf{Y}_1^n}(j, i, \mathbf{y}_1^n) \cdot \log(p_{S_t | S_{t-1}, \mathbf{Y}_1^n}(j | i, \mathbf{y}_1^n)) \\
&= - \sum_{(i,j) \in \mathcal{B}} \sum_{\mathbf{y}_1^n \in \mathcal{Y}^n} p_{S_t, S_{t-1}, \mathbf{Y}_1^n}(j, i, \mathbf{y}_1^n) \cdot \left( \log \left( \frac{p_{S_t, S_{t-1}, \mathbf{Y}_1^n}(j, i, \mathbf{y}_1^n)}{p_{\mathbf{Y}_1^n}(\mathbf{y}_1^n)} \right) - \log \left( \frac{p_{S_{t-1}, \mathbf{Y}_1^n}(i, \mathbf{y}_1^n)}{p_{\mathbf{Y}_1^n}(\mathbf{y}_1^n)} \right) \right) \\
&= - \sum_{(i,j) \in \mathcal{B}} \mu_i p_{ij} \cdot \sum_{\mathbf{y}_1^n \in \mathcal{Y}^n} \left( p_{\mathbf{Y}_1^n | S_{t-1}, S_t}(\mathbf{y}_1^n | i, j) \cdot \log(p_{S_{t-1}, S_t | \mathbf{Y}_1^n}(i, j | \mathbf{y}_1^n)) \right. \\
&\quad \left. - p_{\mathbf{Y}_1^n | S_{t-1}}(\mathbf{y}_1^n | i) \cdot \log(p_{S_{t-1} | \mathbf{Y}_1^n}(i | \mathbf{y}_1^n)) \right) \\
&= - \sum_{(i,j) \in \mathcal{B}} \mu_i p_{ij} \cdot \sum_{\mathbf{y}_1^n \in \mathcal{Y}^n} \left( \frac{p_{S_{t-1}, S_t | \mathbf{Y}_1^n}(i, j | \mathbf{y}_1^n)}{\mu_i p_{ij}} \cdot p_{\mathbf{Y}_1^n}(\mathbf{y}_1^n) \cdot \log(p_{S_{t-1}, S_t | \mathbf{Y}_1^n}(i, j | \mathbf{y}_1^n)) \right. \\
&\quad \left. - \frac{p_{S_{t-1} | \mathbf{Y}_1^n}(i | \mathbf{y}_1^n)}{\mu_i} \cdot p_{\mathbf{Y}_1^n}(\mathbf{y}_1^n) \cdot \log(p_{S_{t-1} | \mathbf{Y}_1^n}(i | \mathbf{y}_1^n)) \right) \\
&= - \sum_{(i,j) \in \mathcal{B}} \mu_i p_{ij} \cdot \left( \sum_{\mathbf{y}_1^n \in \mathcal{Y}^n} p_{\mathbf{Y}_1^n}(\mathbf{y}_1^n) \cdot \log \left( \frac{p_{S_{t-1}, S_t | \mathbf{Y}_1^n}(i, j | \mathbf{y}_1^n)^{p_{S_{t-1}, S_t | \mathbf{Y}_1^n}(i, j | \mathbf{y}_1^n) / \mu_i p_{ij}}}{p_{S_{t-1} | \mathbf{Y}_1^n}(i | \mathbf{y}_1^n)^{p_{S_{t-1} | \mathbf{Y}_1^n}(i | \mathbf{y}_1^n) / \mu_i}} \right) \right),
\end{aligned}$$

with an analogous expression for  $H(S_t | \mathbf{Z}_1^n, S_{t-1})$ , along with using (4) and (5).

## APPENDIX C

## PROOF OF LEMMA 26

Besides the assumptions on the parameterizations  $\mathbf{Q}(\theta)$  made in Assumption 22, we will also assume that for all  $(i, j) \in \mathcal{B}$ , the functions  $Q_{ij}(\theta)$  and  $\mu_i(\theta)$  are affine functions of  $\theta$ , which implies that

$$Q_{ij}^{\theta\theta}(\theta) = 0, \quad \mu_i^{\theta\theta}(\theta) = 0, \quad (15)$$

where the superscript  $\theta\theta$  denotes the second-order derivative w.r.t.  $\theta$ .

Denoting the second-order derivative of  $\bar{\psi}_{\tilde{\mathbf{Q}}}(\theta)$  by  $\bar{\psi}_{\tilde{\mathbf{Q}}}^{\theta\theta}(\theta)$ , we observe that the claim in the lemma statement is equivalent to  $\bar{\psi}_{\tilde{\mathbf{Q}}}^{\theta\theta}(\theta) \geq 0$  for all possible parameterizations of  $\mathbf{Q}(\theta)$  that satisfy the above-mentioned conditions.

Some straightforward calculations show that

$$\bar{\psi}_{\tilde{\mathbf{Q}}}^{\theta\theta}(\theta) = \kappa^2 \kappa' \cdot \left( \sum_{(i,j) \in \mathcal{B}} \frac{(Q_{ij}^\theta)^2}{Q_{ij}} - \sum_{i \in \mathcal{S}} \frac{(\mu_i^\theta)^2}{\mu_i} \right) = \kappa^2 \kappa' \cdot \sum_{i \in \mathcal{S}} \left( \left( \sum_{j \in \tilde{\mathcal{S}}_i} \frac{(Q_{ij}^\theta)^2}{Q_{ij}} \right) - \frac{(\mu_i^\theta)^2}{\mu_i} \right).$$

Noting that for any  $i \in \mathcal{S}$  it holds that

$$\sum_{j \in \tilde{\mathcal{S}}_i} \frac{(Q_{ij}^\theta)^2}{Q_{ij}} = \mu_i \cdot \sum_{j \in \tilde{\mathcal{S}}_i} \frac{Q_{ij}}{\mu_i} \cdot \left( \frac{Q_{ij}^\theta}{Q_{ij}} \right)^2 \geq \mu_i \cdot \left( \sum_{j \in \tilde{\mathcal{S}}_i} \frac{Q_{ij}}{\mu_i} \cdot \frac{Q_{ij}^\theta}{Q_{ij}} \right)^2 = \frac{1}{\mu_i} \cdot \left( \sum_{j \in \tilde{\mathcal{S}}_i} Q_{ij}^\theta \right)^2 = \frac{(\mu_i^\theta)^2}{\mu_i},$$

where the inequality follows from Jensen's inequality. Combining the above two display equations, we can conclude that, indeed,  $\bar{\psi}_{\tilde{\mathbf{Q}}}^{\theta\theta}(\theta) \geq 0$ .

## APPENDIX D

## PROOF OF PROPOSITION 28

Maximizing  $\psi_{\tilde{\mathbf{Q}}}(\mathbf{Q})$  over  $\mathbf{Q} \in \mathcal{Q}(\mathcal{B})$  means to optimize a differentiable, concave function over a polytope. We therefore set up the Lagrangian

$$L \triangleq \sum_{(i,j) \in \mathcal{B}} Q_{ij} \cdot (\tilde{T}_{ij}^B - \tilde{T}_{ij}^E) - \bar{\psi}_{\tilde{\mathbf{Q}}}(\mathbf{Q}) + \lambda \cdot \left( \sum_{(i,j) \in \mathcal{B}} Q_{ij} - 1 \right) + \sum_{(i,j) \in \mathcal{B}} \lambda_j Q_{ij} - \sum_{(i,j) \in \mathcal{B}} \lambda_i Q_{ij}.$$

Note that at this stage we omit Lagrangian multipliers w.r.t. the constraints  $Q_{ij} \geq 0$ ,  $(i, j) \in \mathcal{B}$ . We will make sure at a later stage that these constraints are satisfied thanks to the choice of  $\kappa$  in (13).

Recall that we assume that the surrogate function takes on its maximal value at  $\mathbf{Q} = \mathbf{Q}^*$ .

Therefore, setting the gradient of  $L$  equal to the zero vector at  $\mathbf{Q} = \mathbf{Q}^*$ , we obtain

$$\begin{aligned} 0 &= \frac{\partial L}{\partial Q_{ij}} \bigg|_{\mathbf{Q}=\mathbf{Q}^*} = \tilde{T}_{ij}^B - \tilde{T}_{ij}^E - \frac{\partial \bar{\psi}_{\tilde{\mathbf{Q}}}(\mathbf{Q})}{\partial Q_{ij}} \bigg|_{\mathbf{Q}=\mathbf{Q}^*} + \lambda^* + \lambda_j^* - \lambda_i^*, \quad (i, j) \in \mathcal{B}, \\ 0 &= \frac{\partial L}{\partial \lambda} \bigg|_{\mathbf{Q}=\mathbf{Q}^*} = \sum_{(i, j) \in \mathcal{B}} Q_{ij}^* - 1, \\ 0 &= \frac{\partial L}{\partial \lambda_i} \bigg|_{\mathbf{Q}=\mathbf{Q}^*} = \sum_{r \in \overleftarrow{\mathcal{S}}_i} Q_{ri}^* - \sum_{j \in \overrightarrow{\mathcal{S}}_i} Q_{ij}^*, \quad i \in \mathcal{S}, \end{aligned} \quad (16)$$

where

$$\begin{aligned} \frac{\partial \bar{\psi}_{\tilde{\mathbf{Q}}}(\mathbf{Q})}{\partial Q_{ij}} \bigg|_{\mathbf{Q}=\mathbf{Q}^*} &= \kappa' \cdot \left( \kappa \cdot \log(1 + \kappa \cdot (\delta Q)_{ij}) - \kappa \cdot \log(1 + \kappa \cdot (\delta \mu)_i) \right) \bigg|_{\mathbf{Q}=\mathbf{Q}^*} \\ &= \kappa \cdot \kappa' \cdot \log \left( \frac{(1 - \kappa) \cdot \tilde{Q}_{ij} + \kappa \cdot Q_{ij}^*}{(1 - \kappa) \cdot \tilde{\mu}_i + \kappa \cdot \mu_i^*} \cdot \frac{\tilde{\mu}_i}{\tilde{Q}_{ij}} \right) \\ &= \kappa \cdot \kappa' \cdot \log \left( \frac{\hat{Q}_{ij}^*}{\hat{\mu}_i^*} \cdot \frac{\tilde{\mu}_i}{\tilde{Q}_{ij}} \right) = \kappa \cdot \kappa' \cdot \log(\hat{p}_{ij}^*) - \kappa \cdot \kappa' \cdot \log(\tilde{p}_{ij}). \end{aligned} \quad (17)$$

Here the third and fourth equality use  $\{\hat{Q}_{ij}^*\}_{(i, j) \in \mathcal{B}}$ , which is defined by

$$\hat{Q}_{ij}^* \triangleq (1 - \kappa) \cdot \tilde{Q}_{ij} + \kappa \cdot Q_{ij}^*, \quad (i, j) \in \mathcal{B}, \quad (18)$$

along with  $\{\hat{\mu}_i^*\}_{i \in \mathcal{S}}$  and  $\{\hat{p}_{ij}^*\}_{(i, j) \in \mathcal{B}}$ , which are derived from  $\{\hat{Q}_{ij}^*\}_{(i, j) \in \mathcal{B}}$  in the usual manner.

Note that

$$\begin{aligned} \hat{\mu}_i^* &= (1 - \kappa) \tilde{\mu}_i + \kappa \mu_i^*, \quad i \in \mathcal{S}, \\ \hat{p}_{ij}^* &= \frac{\hat{Q}_{ij}^*}{\hat{\mu}_i^*} = \frac{(1 - \kappa) \cdot \tilde{Q}_{ij} + \kappa \cdot Q_{ij}^*}{(1 - \kappa) \cdot \tilde{\mu}_i + \kappa \cdot \mu_i^*} = \frac{(1 - \kappa) \cdot \tilde{Q}_{ij} + \kappa \cdot Q_{ij}^*}{(1 - \kappa) \cdot \tilde{\mu}_i + \kappa \cdot \sum_{j' \in \overrightarrow{\mathcal{S}}_i} Q_{ij'}^*}, \quad (i, j) \in \mathcal{B}. \end{aligned} \quad (19)$$

Note also that solving (18) for  $Q_{ij}^*$  results in

$$Q_{ij}^* = \frac{1}{\kappa} \cdot (\hat{Q}_{ij}^* - \tilde{Q}_{ij} + \kappa \cdot \tilde{Q}_{ij}), \quad (i, j) \in \mathcal{B},$$

which shows that  $Q_{ij}^* \geq 0$ ,  $(i, j) \in \mathcal{B}$ , for  $\kappa$  satisfying (13). (Recall that when setting up the Lagrangian, we omitted the Lagrange multipliers for the constraints  $Q_{ij} \geq 0$ ,  $(i, j) \in \mathcal{B}$ ; therefore we have to verify that the solution satisfies these constraints, which it does indeed.)

Combining (16) and (17) and solving for  $\hat{p}_{ij}^*$  results in

$$\hat{p}_{ij}^* = \tilde{p}_{ij} \cdot \exp\left(\frac{\tilde{T}_{ij}^B - \tilde{T}_{ij}^E + \lambda^* + \lambda_j^* - \lambda_i^*}{\kappa\kappa'}\right), \quad (i, j) \in \mathcal{B}.$$

Using (11) and defining  $\rho \triangleq \exp\left(-\frac{\lambda^*}{\kappa\kappa'}\right)$  and  $\boldsymbol{\gamma} = (\gamma_i)_{i \in \mathcal{S}}$ , where  $\gamma_i \triangleq \exp\left(\frac{\lambda_i^*}{\kappa\kappa'}\right)$ , allows the rewriting of this equation as

$$\hat{p}_{ij}^* = \frac{A_{ij}}{\rho} \cdot \frac{\gamma_j}{\gamma_i}, \quad (i, j) \in \mathcal{B}.$$

Because  $\sum_{j \in \vec{\mathcal{S}}_i} \hat{p}_{ij}^* = 1$  for all  $i \in \mathcal{S}$ , summing both sides of this equation over  $j \in \vec{\mathcal{S}}_i$  results in

$$1 = \sum_{j \in \vec{\mathcal{S}}_i} \frac{A_{ij}}{\rho} \cdot \frac{\gamma_j}{\gamma_i}, \quad i \in \mathcal{S},$$

or, equivalently,

$$\rho \cdot \gamma_i = \sum_{j \in \vec{\mathcal{S}}_i} A_{ij} \cdot \gamma_j, \quad i \in \mathcal{S}.$$

This system of linear equations can be written as

$$\mathbf{A} \cdot \boldsymbol{\gamma} = \rho \cdot \boldsymbol{\gamma}.$$

Clearly, this equation can only be satisfied if  $\boldsymbol{\gamma}$  is an eigenvector of  $\mathbf{A}$  with corresponding eigenvalue  $\rho$ . A slightly lengthy calculation (which is somewhat similar to the calculation in [10, Eq. (51)]) shows that

$$\psi_{\tilde{\mathbf{Q}}}(\mathbf{Q}^*) = \log(\rho). \quad (20)$$

As is well known, Perron–Frobenius theory guarantees for an irreducible non-negative matrix that the eigenvalue with largest absolute value is a positive real number, called the Perron–Frobenius eigenvalue. Therefore, in order to maximize the right-hand side of (20) over all eigenvalues of  $\mathbf{A}$ , the eigenvalue  $\rho$  has to be the Perron–Frobenius eigenvalue and  $\boldsymbol{\gamma}$  the corresponding eigenvector.

The proof is concluded by noting that (19) can be rewritten as the system of linear

equations

$$Q_{ij}^* - \hat{p}_{ij}^* \cdot \sum_{j' \in \vec{\mathcal{S}}_i} Q_{ij'}^* = \frac{1 - \kappa}{\kappa} \cdot (\tilde{\mu}_i \hat{p}_{ij}^* - \tilde{Q}_{ij}), \quad (i, j) \in \mathcal{B},$$

which can be used to determine  $\{Q_{ij}^*\}_{(i,j) \in \mathcal{B}}$ , because all other quantities appearing in these equations are either known or have already been calculated.

## REFERENCES

- [1] E. M. Kurtas, *Advanced Error Control Techniques for Data Storage Systems*. Boca Raton, FL, USA: CRC Press, 2005.
- [2] B. Vasić and E. M. Kurtas, *Coding and Signal Processing for Magnetic Recording Systems*. Abingdon: CRC Press, 2004.
- [3] K. E. S. Immink, P. H. Siegel, and J. K. Wolf, “Codes for digital recorders,” *IEEE Trans. Inf. Theory*, vol. 44, no. 6, pp. 2260–2299, Oct. 1998.
- [4] G. G. Raleigh and J. M. Cioffi, “Spatio-temporal coding for wireless communication,” *IEEE Trans. Commun.*, vol. 46, no. 3, pp. 357–366, Mar. 1998.
- [5] K. J. P. Golden, H. Dedieu, *Fundamentals of DSL Technology*. Boca Raton, FL, USA: CRC Press, 2005.
- [6] R. G. Gallager, *Information Theory and Reliable Communication*. New York, NY, USA: John Wiley & Sons, 1968.
- [7] A. Kavčić, X. Ma, and M. Mitzenmacher, “Binary intersymbol interference channels: Gallager codes, density evolution, and code performance bounds,” *IEEE Trans. Inf. Theory*, vol. 49, no. 7, pp. 1636–1652, Jul. 2003.
- [8] R. Blahut, “Computation of channel capacity and rate-distortion functions,” *IEEE Trans. Inf. Theory*, vol. 18, no. 4, pp. 460–473, Jul. 1972.
- [9] S. Arimoto, “An algorithm for computing the capacity of arbitrary discrete memoryless channels,” *IEEE Trans. Inf. Theory*, vol. 18, no. 1, pp. 14–20, Jan. 1972.
- [10] P. O. Vontobel, A. Kavčić, D. M. Arnold, and H.-A. Loeliger, “A generalization of the Blahut-Arimoto algorithm to finite-state channels,” *IEEE Trans. Inf. Theory*, vol. 54, no. 5, pp. 1887–1918, May 2008.
- [11] A. Kavčić, “On the capacity of Markov sources over noisy channels,” in *Proc. IEEE Global Communications Conference*, vol. 5, San Antonio, TX, USA, Nov. 2001, pp. 2997–3001.
- [12] S. Yang, A. Kavčić, and S. Tatikonda, “Feedback capacity of finite-state machine channels,” *IEEE Trans. Inf. Theory*, vol. 51, no. 3, pp. 799–810, Mar. 2005.
- [13] P. O. Vontobel and D. M. Arnold, “An upper bound on the capacity of channels with memory and constraint input,” in *Proc. IEEE Information Theory Workshop*, Cairns, Queensland, Australia, Sep. 2001, pp. 147–149.

- [14] J. Chen and P. H. Siegel, “Markov processes asymptotically achieve the capacity of finite-state intersymbol interference channels,” *IEEE Trans. Inf. Theory*, vol. 54, no. 3, pp. 1295–1303, Mar. 2008.
- [15] A. D. Wyner, “The wire-tap channel,” *The Bell System Technical Journal*, vol. 54, no. 8, pp. 1355–1387, Oct. 1975.
- [16] I. Csiszár and J. Körner, “Broadcast channels with confidential messages,” *IEEE Trans. Inf. Theory*, vol. 24, no. 3, pp. 339–348, May 1978.
- [17] M. Bloch and J. N. Laneman, “On the secrecy capacity of arbitrary wiretap channels,” in *Proc. 46th Annual Allerton Conf. Commun. Control and Computing*, Monticello, IL, USA, Sep. 2008, pp. 818–825.
- [18] M. R. Bloch and J. N. Laneman, “Strong secrecy from channel resolvability,” *IEEE Trans. Inf. Theory*, vol. 59, no. 12, pp. 8077–8098, Dec. 2013.
- [19] T. Han, *Information-Spectrum Methods in Information Theory*. Berlin, Heidelberg: Springer, 2003.
- [20] Y. Sankarasubramaniam, A. Thangaraj, and K. Viswanathan, “Finite-state wiretap channels: Secrecy under memory constraints,” in *Proc. IEEE Information Theory Workshop*, Taormina, Italy, Oct. 2009, pp. 115–119.
- [21] B. Dai, Z. Ma, and Y. Luo, “Finite state Markov wiretap channel with delayed feedback,” *IEEE Trans. Inf. Forensics Secur.*, vol. 12, no. 3, pp. 746–760, Mar. 2017.
- [22] H. Zhang, L. Yu, C. Wei, and B. Dai, “A new feedback scheme for the state-dependent wiretap channel with noncausal state at the transmitter,” *IEEE Access*, vol. 7, pp. 45 594–45 604, Apr. 2019.
- [23] S. Hanoglu, S. R. Aghdam, and T. M. Duman, “Artificial-noise-aided secure transmission over finite-input intersymbol interference channels,” in *Proc. 25th Int. Conf. Telecommun.*, St. Malo, France, Jun. 2018, pp. 346–350.
- [24] D. M. Arnold, H.-A. Loeliger, P. O. Vontobel, A. Kavčić, and W. Zeng, “Simulation-based computation of information rates for channels with memory,” *IEEE Trans. Inf. Theory*, vol. 52, no. 8, pp. 3498–3508, Aug. 2006.
- [25] P. Sadeghi, P. O. Vontobel, and R. Shams, “Optimization of information rate upper and lower bounds for channels with memory,” *IEEE Trans. Inf. Theory*, vol. 55, no. 2, pp. 663–688, Feb. 2009.
- [26] A. Dempster, N. Laird, and D. Rubin, “Maximum likelihood from incomplete data via the EM algorithm,” *Journal of the Royal Statistical Society. Series B (Methodological)*, pp. 1–38, 1977.
- [27] C. F. J. Wu, “On the convergence properties of the EM algorithm,” *The Annals of Statistics*, vol. 11, no. 1, pp. 95–103, 1983.
- [28] W. Xiang and S. Pietrobon, “On the capacity and normalization of ISI channels,” *IEEE Trans. Inf. Theory*, vol. 49, no. 9, pp. 2263–2268, Sep. 2003.
- [29] K. L. Judd, *Numerical Methods in Economics*. London: The MIT Press, 1998.